

**SENSITIVITY ANALYSIS OF C- AND Ku-BAND SYNTHETIC APERTURE
RADAR DATA TO SOIL MOISTURE CONTENT IN A SEMIARID REGION**

by

Edson Eyji Sano

A Dissertation Submitted to the Faculty of the

DEPARTMENT OF SOIL, WATER, AND ENVIRONMENTAL SCIENCE

**In Partial Fulfillment of the Requirements
For the Degree of**

**DOCTOR OF PHILOSOPHY
WITH A MAJOR IN SOIL AND WATER SCIENCE**

In the Graduate College

THE UNIVERSITY OF ARIZONA

1997

THE UNIVERSITY OF ARIZONA ®
GRADUATE COLLEGE

As members of the Final Examination Committee, we certify that we have read the dissertation prepared by EDSON EYJI SANO

entitled SENSITIVITY ANALYSIS OF C- AND Ku-BAND SYNTHETIC APERTURE RADAR DATA TO SOIL MOISTURE CONTENT IN A SEMIARID REGION

and recommend that it be accepted as fulfilling the dissertation requirement for the Degree of DOCTOR OF PHILOSOPHY

<u>Alfredo R. Huete</u> Dr. A.R. Huete	<u>6/30/97</u> Date
<u>Ronald F. Post</u> Dr. D.F. Post	<u>6/3/97</u> Date
<u>M. Moran</u> Dr. M.S. Moran	<u>3 June 97</u> Date
<u>Stuart L. Marsh</u> Dr. S.E. Marsh	 Date
<u>[Signature]</u> Dr. S. Yool	 Date

Final approval and acceptance of this dissertation is contingent upon the candidate's submission of the final copy of the dissertation to the Graduate College.

I hereby certify that I have read this dissertation prepared under my direction and recommend that it be accepted as fulfilling the dissertation requirement.

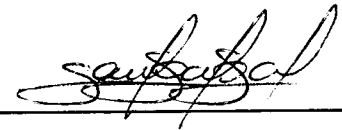
<u>Alfredo R. Huete</u> Dissertation Director	<u>6/30/97</u> Date
--------------------------------------------------	------------------------

STATEMENT BY AUTHOR

This dissertation has been submitted in partial fulfillment of requirements for an advanced degree at The University of Arizona and is deposited in the University Library to be made available to borrowers under rules of the library.

Brief quotations from this dissertation are allowable without special permission, provided that accurate acknowledgement of source is made. Requests for permission for extended quotation from or reproduction of this manuscript in whole or in part may be granted by the head of the major department or Dean of the Graduate College when in his or her judgment the proposed use of the material is in the interests of scholarship. In all other instances, however, permission must be obtained from the author.

SIGNED: _____

A handwritten signature in cursive script, appearing to read "S. Subal", is written over a horizontal line.

ACKNOWLEDGMENTS

Special thanks to my advisor Dr. Alfredo Huete for his guidance, support and patience during the past four years. His 'Remote Sensing of Environment' and 'Monitoring Biosphere' courses taught me the basics of remote sensing. This dissertation would not be completed without his useful suggestions.

I am also grateful to Dr. Post and Dr. Susan Moran. Although they are famous, they always found some time for me. I thank them for sharing their friendship and expertise. I owe special gratitude to my other two committee members, Dr. Stuart Marsh and Dr. Steve Yool, for their comments on my manuscripts and for accepting to be part of my dissertation committee.

Acknowledgments are extended to K. Batchily and J. Qi. They have always been around to solve any of my problems, regardless of Tucson's weather condition. Sincere thanks to Denis Troufleau and Dr. Alain Vidal for their support in the radar image processing at CEMAGREF/ENGREF in Montpellier, France. I appreciate the numerous comments on radar issues from Denis.

A note of thanks for all my folks who helped me in the field and in the laboratory: J. Epiphanio, L. Accioly, G. de Lira, F. Rahman, C. Unkrich, E. Barnes, T. Miura, and S. Mussil.

I am also thankful for the support from Lindy, Judy, Elenor, Barb, and Jan, the staff from the Department of Soil, Water, and Environmental Science.

DEDICATION

To my parents Toyokichi and Shizu (*in memoria*).

I owe my every single accomplishment for them.

To my wife Nilce and my children Naiane, David and Willian,

for their love and support.

TABLE OF CONTENTS

	Page
ABSTRACT	7
1. INTRODUCTION	9
Context of the problem	9
Dissertation format	11
2. PRESENT STUDY	13
Summary	13
Conclusions	17
APPENDIX A: Sensitivity analysis of ERS-1 synthetic aperture radar data to surface moisture content of rocky soils in a semiarid rangeland	18
APPENDIX B: The use of microwave and optical synergism for estimation of soil moisture content from C-band synthetic aperture radar data in a semiarid rangeland	55
APPENDIX C: C- and multi-angle Ku-band synthetic aperture radar data for bare soil moisture estimation in agricultural areas	89

ABSTRACT

In this study, the sensitivity of the C-band (5.3 GHz) with a 23° incidence angle and the Ku-band (14.85 GHz) with 35°, 55°, and 75° incidence angles to surface soil moisture content from a semiarid region were evaluated. To obtain an improved soil moisture estimation, a practical technique to reduce the influence of soil roughness and vegetation in the SAR data was developed in a study area located in the Walnut Gulch Experimental Watershed, a representative site of shrub- and grass-dominated rangelands of the southwestern part of the United States. To correct for soil roughness effects, the C-band radar backscattering coefficients σ° from a wet season image were subtracted from σ° derived from a dry season image. The assumption was that, in semiarid regions, the SAR data from the dry season was dependent only on the soil roughness effects. To correct for vegetation effects, an empirical relation between σ° and leaf area index was used, the latter derived from Landsat Thematic Mapper data. The results showed that when both soil roughness and vegetation effects were corrected for, the sensitivity of σ° to soil moisture improved substantially.

The sensitivity of σ° to soil moisture was also evaluated in agricultural fields with bare soil and periodic roughness components (planting row and furrow structures). Four types of SAR system configurations were analyzed: C-band with a 23° incidence angle and Ku-band with 35°, 55°, and 75° incidence angles. The test sites were located at the University of Arizona's Maricopa Agricultural Center, south of Phoenix, Arizona. The results showed that the sensitivity of σ° to soil moisture was strongly dependent upon the field conditions. The

SAR signals were nearly insensitive to soil moisture for furrowed fields (furrow spacing ~ 95 cm; amplitude ~ 22 cm), but for fields with planting row structures (row spacing ~ 24 cm; amplitude ~ 2 cm), the SAR data were sensitive to soil moisture, particularly with the C-band at a 23° incidence angle and the Ku-band with a 35° incidence angle, regardless of the row direction.

CHAPTER 1

INTRODUCTION

Context of the problem

Soil moisture estimates are important in various environmental sciences such as in agronomy and hydrology. For instance, in agronomy, soil moisture information is used to improve the crop yield prediction and irrigation scheduling, whereas in the hydrologic point of view, soil moisture influences the amount of runoff produced by a given amount of precipitation, at a scale of a watershed. Because of its high spatial and temporal variability, soil moisture data needs to be obtained continuously over large areas and repetitively.

Synthetic aperture radar (SAR) data appear very promising to estimate soil moisture content because of a large contrast between the dielectric constant of liquid water (~ 80) and a dry soil (3-5). However, there are still some major problems in the estimation of soil moisture from SAR data to be addressed. This dissertation addressed three of them:

1. Depending upon the sensor configuration and field condition, SAR data can result in poor estimates of soil moisture. The response of SAR data to soil moisture is coupled with soil roughness and vegetation effects. For example, the effects of soil roughness in the backscattering process can be significant if the SAR system operates at incidence angles larger than 10° , or if the site has a high percent of rock fragments. Thus, the difficulty in soil moisture estimation from rocky soils using available satellite-based SAR data was addressed in this dissertation.

2. The current techniques to account for the influence from vegetation and soil roughness in the SAR data are restricted to specific sensor configurations. They involve either dual-frequency or dual-polarization SAR data, which are unavailable in current satellite-based SAR systems. Thus, a more practical approach to reduce the effects of soil roughness and vegetation was developed in this study, using single polarization and single frequency SAR data.
3. Based on soil moisture data collected from temperate regions, it has been assumed that, over sparsely vegetated areas, the contribution from vegetation in the backscattering process can be neglected; that is, the only important effect of the vegetation in such regions is the attenuation of the radar signal from the soil. However, in arid and semi-arid regions, soil moisture contents hardly exceed 20%, indicating that the contribution from soil in the radar backscattering process may also be small, or at least on the same order of magnitude as the contribution from the vegetation layer. In other words, the contribution from vegetation in the arid and semiarid regions may not be neglected. Thus, the effect of vegetation in SAR data from a semiarid region was investigated and a practical approach to reduce its effect was also developed.

One part of the data analyzed in this dissertation was collected during the WG'92 experiment, conducted in Walnut Gulch Experimental Watershed, southeast of Arizona, from April to November, 1992. This experiment was designed to obtain remote sensing data in the visible, near-infrared, thermal, and microwave spectral regions, with concurrent measurements of soil moisture, biomass, and temperature, among others. Another part of the data was

collected during the Multispectral Airborne Demonstration at the Maricopa Agricultural Center (MADMAC) experiment, in January, 1996. The objective of this experiment was to test the potential of airborne multispectral imagery for farm management purposes.

Dissertation format

The main body of this dissertation consists of three research papers appended to this dissertation. The sensitivity of SAR data to the moisture content from rocky soils was investigated in the first two papers (Appendices A and B). A technique to reduce the soil roughness effects in the SAR data was developed in the first paper, whereas another technique to reduce the effects from vegetation was developed in the second paper. The sensitivity of SAR data (four different system configurations) to the soil moisture content over agricultural areas with periodic row and furrow structures was investigated in the third paper (Appendix C).

In the first paper, the author designed the field campaign, under the guidance of Dr. Alfredo Huete. The radar image was processed at CEMAGREF/ENGREF in Montpellier, France, under supervision of Dr. Alain Vidal and Dr. Denis Troufleau. The data analysis and the write-up of the manuscript was done by the author. The original idea of the second paper was suggested by Jianguo Qi from USDA/ARS. The author was responsible for data processing, data analysis, and writing, under the guidance of Dr. Alfredo Huete. The author designed the experiment for the third paper with the help from Dr. Susan Moran and Dr. Alfredo Huete. Dr. Susan Moran was also responsible for the acquisition of SAR data from

Sandia National Laboratories, Albuquerque, NM and from the Canadian Center for Remote Sensing, Richmond, Canada.

CHAPTER 2

PRESENT STUDY

Summary

The literature review, site descriptions, methods, results, and conclusions of this study are presented in the papers appended to this dissertation. The following is a summary of the most important findings in these papers.

Paper # 1: Active microwave data have demonstrated their potential in the estimation of soil moisture content. However, because the soil moisture response to a specific radar configuration is coupled to vegetation and soil roughness effects, the interaction among all three parameters needs to be investigated. For instance, the difficult estimation of moisture content from rocky soils needs to be addressed, since the effect of a rough surface in synthetic aperture radar (SAR) data is to increase the surface emissivity and thus to decrease the sensitivity to soil moisture.

In this paper, the sensitivity of C-band (5.3 GHz) SAR data to soil moisture contents in rocky from a sparsely vegetated semiarid rangeland was investigated. A practical technique to reduce the effects of soil roughness was developed based on radar data collected during the wet and dry seasons. This technique consisted in a subtraction $\sigma^{\circ}_1 = (\sigma^{\circ}_{\text{wet}} - \sigma^{\circ}_{\text{dry}})$, where σ°_1 is the SAR data corrected for soil roughness effects; and $\sigma^{\circ}_{\text{wet}}$ and $\sigma^{\circ}_{\text{dry}}$ are the radar backscattering coefficients from a wet season and a dry season image, respectively. The assumption was that the C-band SAR data from the dry season in semiarid regions was

dependent only on the contribution from soil roughness.

The linear correlation between C-band data and surface soil moisture content was poor, but improved when the effects from soil roughness in the radar backscattering coefficients were subtracted. Thus, the subtraction technique, if shown to be valid for other semiarid sites, can become an easy way to account for soil roughness effects in SAR data, using a single polarization and single frequency system configuration. Although this technique improved the linear correlation between σ° and soil moisture, it was still lower than those obtained in temperate regions ($r^2 > 0.80$). This low correlation was probably due to the difficulty in sampling moisture in highly spatially variable environments. Consequently, an adequate ground soil moisture sampling scheme would be a key issue in calibration and estimation of soil moisture from SAR data in semiarid regions. The influence from vegetation, which was not corrected in this paper, could also have contributed to the low correlation.

Paper # 2: Research from temperate regions have suggested that vegetation has minimal effects on the SAR signal in sparsely vegetated areas. The sparse vegetation layer only attenuates the soil signal. However, in semiarid regions, the volumetric soil moisture content hardly exceeds 20%, indicating that the contribution from the soil may also be small or at least of the same magnitude of contribution from vegetation. Thus, the contribution from the vegetation may not be neglected.

Microwave and optical synergism was used in this study to verify the effects of the vegetation in the C-band SAR data from a semiarid region. More specifically, multitemporal radar backscattering coefficients σ° derived from the European Remote Sensing (ERS-1)

SAR data were compared with leaf area index (LAI) values obtained from multitemporal Landsat Thematic Mapper data. An empirical linear relationship between σ° and LAI was used to account for the vegetation effects in the SAR data corrected for roughness effects (see description of the method to correct for roughness effects in Paper # 1).

The most significant finding of this paper was that C-band SAR data were highly, positively correlated with multitemporal LAI values, indicating that, in fact, there is contribution from vegetation in the SAR data in semiarid regions. The techniques used in this study to account for soil roughness and vegetation effects resulted in more accurate soil moisture estimates and, upon validation, can be an easy way to obtain improved soil moisture estimates from a single polarization and single frequency SAR data.

Paper # 3: The estimation of soil moisture in agricultural fields is important to improve yield forecasting and irrigation scheduling, among other farm management practices. Indirect soil moisture estimation from remotely sensed data can overcome the limitations of conventional ground-based soil moisture measurement techniques such as the neutron probe, Time Domain Reflectometry, and gravimetric methods, which are essentially point-based measurements at a specific time. The C-band (5.3 GHz) with an incidence angle around 10° has been reported as the optimum configuration for soil moisture. However, such a configuration is not available in the current satellite-based SAR systems, except for the Canadian Remote Sensing (RADARSAT) satellite. For systems operating at incidence angles larger than the above mentioned value, the effects from soil roughness cannot be neglected. Depending upon the combination of frequency and incidence angle, the range of radar

backscattering coefficients σ° due to surface roughness can vary up to 22 decibels (dB). The presence of periodic row or furrow structures in some agricultural fields can also exert considerable angular effects in the radar backscatter process. Thus, the effects of soil roughness for a given sensor configuration and field condition need to be addressed by using either experimental data or theoretical/semiempirical models.

The sensitivity of the C-band (5.3 GHz) with a 23° incidence angle and the Ku-band (14.85 GHz) with 35°, 55°, and 75° incidence angles to soil moisture from agricultural fields with periodic roughness structures were evaluated in this study. The fields presented either a small-scale, periodic roughness structure associated with level-basin irrigation system or an intermediate-scale, periodic roughness structure associated with a furrow irrigation system.

An important finding in this study was that the SAR data was sensitive to soil moisture for fields with a small-scale periodic roughness component, particularly for the C-band with a 23° incidence angle and the Ku-band with a 35° incidence angle. The direction of the small-scale, periodic roughness component did not present any influence in the scattering process, regardless of the frequency and incidence angle. However, for furrowed fields, the SAR data from all configurations were nearly insensitive to soil moisture content. In this case, the relatively large soil clods (more than 15 cm in diameter), randomly distributed in the furrowed fields, most likely played a major role in the backscattering process.

Conclusions

The results of these experiments indicated that the effects of soil roughness and vegetation on the radar backscattering coefficients from semiarid regions are significant and must be reduced to obtain improved soil moisture estimates. A practical technique to reduce these effects were developed in this dissertation, and upon validation, can become an easy way to account for the effects of soil roughness and vegetation from a single frequency and single polarization SAR data. Future research involving more multitemporal data and more vegetation types needs to be conducted to obtain a more generic σ° -LAI relationship for arid and semiarid regions.

APPENDIX A:

Sensitivity Analysis of ERS-1 Synthetic Aperture Radar Data to Surface Moisture Content of Rocky Soils in a Semiarid Rangeland

E.E. Sano¹, A.R. Huete¹, D. Troufleau², M.S. Moran³, A. Vidal²

¹ Department of Soil, Water, and Environmental Science, The University of Arizona, 429 Shantz Bldg # 38, Tucson, AZ, 85721, USA

² LCT CEMAGREF-ENGREF, 500 rue J.F. Breton, 34093 Montpellier, Cedex 5, France

³ USDA-SWRC, 2000 E. Allen Road, Tucson, AZ, 85719, USA

Submitted to "Water Resources Research"

ABSTRACT

This study was conducted to analyze the sensitivity of the European Remote Sensing Satellite (ERS-1) C-band synthetic aperture radar (SAR) data to the surface moisture content of rocky soils in a semiarid rangeland in southeast Arizona. A dry season and a wet season SAR images were corrected for topographic effects. Soil moisture content and soil roughness were obtained from 47 sampling sites. An intensive soil moisture sampling campaign was also conducted at three sites to determine the number of samples necessary to estimate soil moisture content with 10% accuracy. Soil roughness was found to be a dominant factor affecting the backscattering coefficients. A general trend between soil moisture content and SAR data was seen only after the correction of SAR data for soil roughness effects. The number of soil moisture samples were a crucial factor in obtaining representative soil moisture values. In the study area, at least seven samples per acre were needed to obtain soil moisture estimates with 10% accuracy.

INTRODUCTION

One of the major goals in hydrology is to understand and quantify the processes that control hydrologic storage and fluxes at local, regional, and global scales [Moran et al., 1994]. Soil moisture content plays a critical role in these hydrologic processes as an environmental descriptor that integrates much of the land surface hydrology [Engman and Chauhan, 1995]. Thus, this variable needs to be measured consistently on a spatially distributed basis. Ground-based techniques, such as the gravimetric method, neutron probe,

and Time Domain Reflectometry, can provide accurate estimates of soil moisture, but they are labor intensive and essentially represent point-based information of the terrain at a certain time. The highly intermittent character of precipitation as well as the heterogeneity of evapotranspiration, topography and soil physical and chemical properties, such as texture, porosity and structure, create large spatial and temporal variations in soil moisture [Wei, 1995]. As a result, this important variable is often neglected in hydrologic, climatic, and agricultural models.

Many researchers [Ulaby and Batlivala, 1976; Bertuzzi et al., 1992; Rao et al., 1993; Taconet et al., 1996] have studied the potential of remotely sensed data to estimate surface soil moisture contents, mainly at centimeter wavelengths (microwave spectral region), with the aim of obtaining multitemporal soil moisture information over large areas. Experiments with truck-, aircraft-, and spacecraft-mounted microwave sensors have shown good predictions of soil moisture within the top 5 centimeters. However, these promising results were obtained over agricultural fields with homogeneous crop cover and surface roughness, flat surfaces, and wide ranges of soil moisture as well as in watersheds located mostly in temperate climates with a high range (10–40 %) of volumetric soil moisture contents [Bernard et al., 1982; Benallegue et al., 1994; Cognard et al., 1995]. As pointed out by Engman and Chauhan [1995], the difficult task of soil moisture retrieval from rocky soils needs to be addressed. The high percent of rock fragments increases the influence of soil roughness on the radar backscattered signals, making the retrieval of soil moisture contents difficult.

The objective of this study was to conduct a sensitivity analysis of radar backscattered

energy in the C-band (5.3 GHz) to the surface moisture content of rocky soils from the Walnut Gulch Experimental Watershed (31.72° N latitude, 110.00° W longitude), located in a semiarid rangeland in Tombstone, Arizona (Figure 1). The influence of soil roughness in the synthetic aperture radar (SAR) data and the number of samples necessary to obtain moisture content estimates with 10% accuracy were also addressed in this experiment.

BACKGROUND

The microwave region (from 1 millimeter to 1 meter) has been the most promising spectral region for soil moisture measurements [John, 1992]. Microwave data is sensitive to soil moisture content because of the large contrast between the dielectric constant of liquid water (approximately 80) and dry soil (3-5) [Ulaby et al., 1986]. Thus, as the soil moisture increases, even slightly, the dielectric constant can increase to a value of 20 or greater [Schmugge, 1983, 1985]. Other strengths of the microwave sensors are their capacities of day/night operation, cloud penetration, and large-scale mapping within a short period of time, and reasonable cost [Schmullius and Furrer, 1992a].

Optimum sensor configuration for soil moisture study

Some authors [Ulaby et al., 1979; Bernard et al., 1982; Jackson and O'Neil, 1985; Brisco et al., 1991] have reported that the C-band (5.3 GHz) was the best wavelength to estimate soil moisture from SAR data. They showed that the correlation between the backscattered signal and soil moisture was less ambiguous for C-band than for shorter

frequencies such as L-band (1.25 GHz) because of the high sensitivity of the radar backscattering signal to soil roughness at this frequency. For sensors operating at relatively large frequencies, such as the X- (9 GHz) and Ku- (15 GHz) bands, the backscattering from the vegetation layer is higher than from the soil layer because of the relatively weak penetration capacity of the radar signals into the canopy.

The optimal incidence angles for soil moisture studies are from 7° to 10° [Ulaby and Batlivala, 1976; Ulaby et al., 1978, 1979]. Within this range, the effects of soil roughness and vegetation absorption and diffusion are minimal. However, spacecraft platforms require larger incidence angles to obtain a high range of spatial resolutions [Autret et al., 1989; Bertuzzi et al., 1992]. Thus, all satellites currently carrying active microwave sensors have incidence angles larger than 15° : ERS-1 and ERS-2 (European Remote Sensing Satellite, 23° incidence angle); JERS-1 (Japanese Earth Resources Satellite, 38° incidence angle); and RADARSAT-1 (Canadian Remote Sensing Satellite, 20° - 49° incidence angle, standard mode). With respect to the polarization type, Schmullius and Furrer [1992b] reported that H- polarization for the receiving channel, that is, the second 'H' in the HH or VH notation, is more sensitive to soil moisture than the V- polarization. The V- polarization for the receiver is more sensitive to surface wetness of the plants than to soil moisture.

Semiempirical backscattering model

One major difficulty in mapping soil moisture using microwave sensors is the influence from both the vegetation canopy and soil roughness. For instance, agricultural fields with

furrows oriented perpendicular to the radar incident direction or sites with a high percent of rock fragments can result in a low correlation between the radar backscattering coefficient (σ^0) and soil moisture. A model known as 'water-cloud' [Attema and Ulaby, 1978; Mo et al., 1984; Bouman, 1991; Prevot et al., 1993a, 1993b] is commonly used to analyze the radar backscattering coefficient σ^0 of the canopy in terms of the contribution from vegetation σ^0_{veg} and soil σ^0_{soil} layers:

$$\sigma^0 = \sigma^0_{veg} + \tau^2 \sigma^0_{soil} \quad (\text{units: } m^2/m^2) \quad (1)$$

where τ^2 is the two-way attenuation of the vegetation layer.

In the C-band, the scattering contribution by the vegetation volume (σ^0_{veg}) is significant only at high levels of biomass, such as dense crops and tropical and temperate forests. For semiarid regions, where the biomass is less than 1 kg/m^2 , the σ^0_{veg} factor can be considered negligible. Therefore, the two-way attenuation τ^2 (units = m^2/m^2), which is primarily due to the vegetation water content, is the only effect to take into account from vegetation in semiarid regions [Troufleau et al., 1994]. This attenuation factor was given by Prevot et al. [1993a, 1993b]:

$$\tau^2 = \exp\left[\frac{-2 B m_v}{\cos \alpha}\right] \quad (2)$$

where B is a constant related to the canopy type and canopy structure for a given radar configuration, m_v is the vegetation water content, and α is the incidence angle.

The soil contribution $\sigma_{\text{soil}}^{\circ}$ (units = decibels, dB) is usually expressed as a linear function of its volumetric soil moisture content h_v [Ulaby et al., 1978; Dobson and Ulaby, 1981; Bernard et al., 1982; Bruckler et al., 1988; Prevot et al. 1993a, 1993b]:

$$\sigma_{\text{soil}}^{\circ} = C + D h_v \quad (\text{units: dB}) \quad (3)$$

where C is a roughness dependent parameter and D is a constant.

Based on these three functions and on unit conversion, Eq. (1) can be rewritten by:

$$\sigma^{\circ} = \frac{-B' m_v}{\cos \alpha} + C + D h_v \quad (\text{units: dB}) \quad (4)$$

where

$$B' = \left[\frac{20}{\ln 10} \right] B$$

This equation shows the following relationships between the scattering process and the surface biophysical parameters:

a) decrease of σ° with an increase of vegetation water content (m_v , attenuation effect), for

- a given sensor incidence angle α ;
- b) increase of σ° with an increase of soil surface roughness, controlled by the C parameter;
and
- c) increase of σ° with an increase of soil moisture content (h_v).

EXPERIMENTAL DESIGN

Study area

The Walnut Gulch Experimental Watershed has been operated by the U.S. Department of Agriculture (USDA) Agricultural Research Service (ARS) since 1954. The predominant textures of surface soils (0-5 cm) are gravelly loamy sands and sandy loams, with a small quantity of organic matter and a rock content around 30% [Gelderman, 1970; Kustas and Goodrich, 1994]. The vegetation is a mixed shrub/grass rangeland; that is, shrub-dominated in the western part of the watershed, while the eastern part is dominated by grass (Figure 1).

Radar images

This report was based on analyses of two ERS-1 SAR images acquired by the European Space Agency (ESA). The ERS-1 satellite carries a SAR sensor operating at 5.3 GHz (C-band), VV polarization, 23° incidence angle, 100 km swath width, and 12.5 meters pixel spacing. One wet season image was acquired in late July, 1994 [Day of Year (DOY) 206]. This date was chosen to obtain a scene with high field soil moisture content during the

satellite overpass. Normally, about two thirds of the rainfall in the watershed occur as high intensity, convective thunderstorms during the 'monsoon' season in July and August. The mean annual precipitation typically ranges from 250 to 500 mm per year. Based on the records from 89 raingages located in the watershed, the first storm associated with the summer 'monsoon' season on DOYs 204 and 205, 1994 produced an average precipitation of 10.3 mm (standard deviation = 3.1 mm). Another image previously acquired in the middle of May, 1992 (DOY 116) as part of the WG'92 experiment [Moran et al., 1996] was also analyzed. This image was obtained in the dry season, when the surface was dry and covered with senescensed vegetation.

These images corresponded to the standard Precision Image products (PRI), which were corrected for antenna elevation, gain pattern, and range spreading loss [Cognard et al., 1995]. They were also georeferenced to the Universal Transverse Mercator (UTM) coordinate system (Zone 12, 1927 North American Datum, Clarke 1866), corrected for topographic effects, and calibrated, that is, corrected to account for the real backscattering area of each pixel, using a DEM [Beaudoin et al., 1994]. The elevation model was derived from topographic maps in 1:24,000 scale with a contour interval of 6.1 meters. Radar backscatter coefficients (σ°) were extracted from these preprocessed images using the following equation :

$$\sigma^{\circ} = 10 \log \left[(\overline{DN})^2 + STD^2 / K \right] \quad (\text{units : dB}) \quad (5)$$

where DN = digital number;
STD = standard deviation; and
K = system calibration constant.

In this study, we used approximately 200 pixels per site to obtain the DN values. Bruniquel [1996] showed that with this number of pixels, σ° values are expected to be within a confidence interval smaller than 1 dB. In fact, all sites presented confidence intervals smaller than 0.8 dB.

Ground-Based Measurements

Soil samples for gravimetric moisture measurements within the top 5 cm (three replicates) were collected on the same day of the 1994 satellite overpass under two different surface conditions (Figure 2). One set of 26 sites were located in the eastern grass-dominated part of the watershed, over the very gravelly sandy loam Elgin-Stronghold Complex soil unit [Breckenfeld, 1993]. Another set of 21 sites were located at the western shrub-dominated part of the watershed, a very gravelly sandy loam Luckyhills-McNeal complex soil unit. These soil types represent, respectively, the most extensive soil mapping units in the grass-dominated and shrub-dominated areas in the watershed (Table 1). Dry bulk density data were also obtained for each sampling point (three replicates) by the excavation method [Blake and Hartge, 1986], allowing the calculation of volumetric soil moisture.

Soil surface roughness measurements were made using a roughness meter developed by Simanton et al. [1978], which measures 100 heights of soil surface per meter. Three plots

each, having an area of $1 \times 2\text{m}^2$, were randomly selected per site. The roughness meter, aligned every 20 cm interval, gave us 3000 point readings per site. These points were connected to lines and digitized using a GIS software package (Arc/Info) to calculate the average standard deviation (in centimeters). This average corresponded to the roughness index or to the root mean square (RMS) height variation of the site.

Percent rock fragment and dry biomass were also measured within a month, following the 1994 satellite overflight at 18 sites (10 in the grass-dominated areas and 8 in the shrub-dominated areas). The percent rock fragment was determined with the line-intercept transect method [Canfield, 1941]. Two lines with 100 meter extensions were chosen randomly for each site. The percent rock fragment (more than 5 mm in diameter) was calculated from the following ground characteristics recorded at 1 m-interval along these transects: bare soil, rock fragment, grass, shrub, forb, and litter. Five $1 \text{ m} \times 0.5 \text{ m}$ areas were selected along the transect, spaced by 20 m. All the green vegetation and litter within these areas were clipped, collected, oven-dried at 60°C for 24 hours and weighed to determine the dry biomass (kg/m^2).

The following additional soil physical and topographic data were also obtained for most of the sites: slope, % gravel, % clay, and % sand. The slopes corresponded to the average of two soil scientist estimates in the field. They also determined the correct soil series for each site. The % gravel was obtained by collecting 1 liter of soil sample at 0-5 cm depth, removing the fine particles ($< 5 \text{ mm}$) by sieving, and estimating its remaining volume in a 1-liter Erlenmeyer flask. The % clay and % sand were estimated in the laboratory by manipulating the soil samples in the hand. The soil texture was estimated by more than 40

students taking a Soil Morphologic, Classification, and Survey class offered by the University of Arizona (Fall Semester of 1996).

Another field soil moisture campaign was conducted on November 4, 1996 (DOY 309, 1996) at three sites with different topographies (flat, north-faced slope, and hilly-shaped slope). The location of these sites are shown in Figure 2. Sixty four gravimetric soil moisture samples were taken at a regular 20 m-spaced grid within a 100-m radius area. The purpose of these measurements was to estimate the number n of samples required to obtain moisture content data with acceptable accuracy. The following data are required to calculate n : coefficient of variation CV (ratio of the standard deviation to the mean value) from the field measurements; confidence level; and the percent of maximum allowable error d , which indicates the expected closeness of the sample mean \bar{x} to the population mean μ [Warrick et al., 1996]. These parameters are related by:

$$n = \frac{t^2 (CV)^2}{d^2} \quad (6)$$

where t is a constant that depends on the confidence level and is obtained from a statistical table (t-test, degree of freedom = ∞). The assumption is that the soil moisture measurements for the study area has a normal distribution function.

RESULTS AND DISCUSSION

Sensitivity of C-band SAR data to the soil moisture variation

Tables 2 and 3 summarize the SAR data and the surface biophysical properties at each sampling location. The sensitivity of the C-band SAR data to the soil moisture content variation was analyzed by plotting the radar signals from the wet season against the signals from the dry season images (Figure 3). Most of the points are located above the 1:1 line, indicating that the backscattering coefficients of the wet season are higher than those of dry season. The average variation of σ° between these two dates for grass and shrub-dominated sites was 1.0 dB (maximum = 2.3 dB) and 1.2 dB (maximum = 2.4 dB), respectively.

This higher backscattering coefficients for the wet season image were due to an overall higher soil moisture condition. The soil roughness remained essentially the same within the two dates. In contrast to agricultural fields, soil roughness does not change significantly over relatively short time periods in natural ecosystems. The vegetation condition was approximately similar for both satellite overpasses, since the July 23 and 24, 1994 rainfall was the first rainfall associated with the 'monsoon' event. Thus, the vegetation was mostly dry for both overflights. The vegetation water content was probably slightly higher in the 1994 image, especially at the shrub-dominated sites, but the effect on the radar signal is attenuation, not addition (see Eq. 4). Therefore, the higher radar backscattering signals in the wet season image were most likely due to the higher soil moisture condition.

Sensitivity of C-band SAR data to the soil roughness

The sensitivity of the C-band SAR data to soil roughness is shown in the scatterplot between RMS height and σ° of the dry 1992 satellite overpass (Figure 4). The roughness was considered the only surface parameter influencing the backscattering process on this date because of the dry condition. Thus, a variation of approximately 1.5 cm in RMS height (from 0.5 to 2.0 cm) induced a σ° variation of approximately 2.5 dB in the grass-dominated data set (Figure 4a). For the shrub-dominated data set, the σ° variation was on the order of 3.5 dB for a RMS height variation of 1.5 cm (Figure 4b). Thus, the σ° variation due to soil roughness was higher than the average σ° variation caused by soil moisture differences (see Figure 3).

The relationship between radar backscattering coefficients and soil roughness was described by an exponential function. The coefficients of determination obtained for both grass- and shrub-dominated data sets were relatively high: $r^2 = 0.83$ for grass-dominated areas and 0.90 for shrub-dominated areas. Altese et al. [1996] also found an exponential correlation between these two parameters, indicating that the sensitivity of radar data to soil roughness is stronger at lower roughness conditions. Thus, the radar backscattered energy due to the soil roughness can be determined successfully from a dry season overpass.

An analysis of partial correlation coefficients (Table 4) also showed a higher contribution of soil roughness ($r = 0.45$ and 0.64 for grass and shrub-dominated sites, respectively) in comparison to the contribution of soil moisture ($r = -0.18$ and 0.46 , respectively). Partial correlation is the correlation between two variables with the effects of a third cancelled out [Kline, 1994]. The correlation between σ° and soil moisture was very

low for grass-dominated sites. The negative signal indicates an inverse relationship between these two parameters, which is the opposite of the radar backscattering theory. Jackson and Schmugge [1991] also found that grass-covered sites have an unusual behavior compared to other vegetation types. The accentuated accumulation of litter and stubble on the soil surface is likely to produce a significant attenuation in the SAR signal when filled with water; that is, immediately after a rainfall event, masking the contribution from the underlying soil moisture content.

Relationship between SAR data and soil moisture after correcting for soil roughness effects

In this section, the relationship between σ° and soil moisture content was analyzed by accounting for the effects of soil roughness. One approach is to use the co-polarization ratio technique (the ratio between SAR data acquired by HH polarization and VV polarization simultaneously). Experimental and modeled data from this dual-polarization configuration (e.g. Autret et al., 1989) have indicated that the final product is nearly insensitive to the roughness parameter. However, all satellites currently carrying a SAR sensor have acquired only single-polarized data.

In this study, the differences in the σ° between the wet season and a dry season images were compared with the volumetric soil moisture data. The difference is equivalent to the subtraction of the C term in the Eq. (4). This approach, known as the change detection technique, seems to be a reasonable way to detect changes in the dielectric properties of soil

surfaces by removing the roughness and vegetation effects without using multifrequency or multipolarization configurations. The following are the assumptions: a) the DOY 116 image is only function of the roughness parameter; b) the soil roughness did not change between the two overpasses; c) the vegetation condition in the study area was the same in the two overpasses; and d) the calibration and the geometric registration of the two images were accurate.

A linear regression analyses between σ° differences and soil moisture content for the two data sets did not present any significant correlation at a level of significance $\alpha = 0.10$. Nevertheless, a general increasing trend was found after removing the points without replicates of soil moisture samples in the grass-dominated sites or after removing the sites with the coefficient of variation of gravimetric soil moisture content higher than 0.15 in the shrub-dominated sites (Figure 5). Such a trend was not found when the soil moisture was compared with the wet season SAR data, without subtracting the signal from the dry season image (Figure 5). This indicated that the change detection technique improved the relationship between σ° and the soil moisture by removing the roughness effects, but the relationship was not as good as expected ($r^2 = 0.12$ and 0.31 for grass-dominated and shrub-dominated sites, respectively). The major factor for the dispersion of the points was probably due to the high spatial variability of soil moisture. Therefore, an adequate ground soil moisture sampling to represent its high spatial variability is a key issue for the analysis of relationship between σ° and h_v .

Calculation of required optimal number of samples

Table 5 indicates the optimal number of soil samples for three grass-dominated sites with three different slopes, considering a maximum allowable error $d = 0.1$ and a confidence level of 99%. The d value can be considered as the maximum acceptable error for hydrologic applications, which requires soil moisture measurements with an accuracy within a few percent [Houser et al., 1996]. As mentioned, each site corresponded to an area (circle) with 100 m radius (approximately 7.75 acres). It is evident that the number of samples was strongly dependent upon the slope. For relatively flat surfaces, the calculated number of samples was 60 (about 7 samples per acre), whereas for a hilly-shaped slope, the number increased to 193 (about 25 samples per acre). Thus, the poor correlation between σ° and soil moisture obtained for 1994 data set was probably due to an insufficient number of soil samples.

Considering that these numbers were calculated using data obtained in the winter season, the number of samples would be even higher in the 'monsoon' season because of the higher rate of evaporation. In other words, these optimal numbers of samples can be strongly season- and site-specific. The spatial variability of soil moisture at a given site depends on the slope as well as other parameters, such as vegetation density, soil textural class and amount of precipitation. Rao and Ulaby [1977] also obtained different n values for random and stratified sampling methods. Thus, additional analyses at other sites in the watershed is recommended.

CONCLUDING REMARKS AND SUMMARY

This study reported a sensitivity of the C-band SAR data to the moisture content and roughness of rocky soils in the semiarid Walnut Gulch Experimental Watershed, Tombstone, AZ. The sensitivity of the C-band SAR data to soil roughness was found to be higher than the sensitivity to soil moisture. Thus, the influence of soil roughness must be corrected to accurately estimate soil moisture with SAR images. The correction can be made using a dry season image. The scatterplot between the 1992 radar backscattering coefficients and RMS heights showed a high exponential correlation, indicating that the RMS height parameter was a good descriptor of soil roughness. This exponential function can be used to determine the contribution of roughness to the backscattering process. Another technique is the use of the 'difference' between wet season and dry season images. Considering that the roughness and the vegetation conditions remained approximately the same in both seasons, the σ° (dB) from the difference can be considered a function of soil moisture variation. This change detection technique is a simple technique to reduce the influence of roughness and vegetation, using both single polarization and single frequency sensor configuration. However, the correlation between σ° difference and soil moisture was not as high as expected probably due to the high spatial variability of soil moisture. In this study, the sampling size analysis indicated that at least seven samples per acre were required to represent the watershed's soil moisture content with a 10% accuracy.

Another factor which could have contributed to the poor correlation between σ° and soil moisture was the relatively large sampling time interval (8:00 AM - 5:00 PM, local time)

for this experiment, because of the relatively poor road conditions and limited number of personnel available. Soil samples taken early in the morning or late in the afternoon may have presented moisture contents significantly different from that recorded by the sensor. A differentiated attenuation in the backscattering process is also expected as a function of different biomass among the sampling sites (see Tables 2 and 3).

ACKNOWLEDGMENTS

Special thanks are due to J. Epiphanio, L. Accioly, F. Rahman, C. Unkrich, G. de Lira, and K. Batchily for helping us in the field work; Dr. D.F. Post and D. Breckenfeld for checking the soil units and collecting the soil morphology data from most of the field sites; Dr. S. Marsh and Dr. J. Qi for reviewing the manuscript; and Dr. A.W. Warrick and S. Musil for permitting us to use their Soil Physics Lab at the University of Arizona to obtain soil moisture measurements. We also greatly appreciated the cooperation of people from USDA Southwest Watershed Research Center, Tucson, AZ: Dr. M. Wertz for his orientation in vegetation sampling technique, Dr. D. Goodrich for providing the orthophotos of the watershed, and R. Simanton for allowing the use of the roughness meter. The assistance of personnel at the ARS Walnut Gulch Experimental Watershed facility in Tombstone, AZ, was also very important. This work was partially supported by the NASA-EOS Interdisciplinary Research Program in Earth Sciences (NASA IDP-88-086) and National Science Foundation grant (INT-9314872).

REFERENCES

- Altese, E., O. Bolognani, and M. Mancini, Retrieving soil moisture over bare soil from ERS 1 synthetic aperture radar data: sensitivity analysis based on a theoretical surface scattering model and field data. *Water Resour. Res.*, 32(3), 653-661, 1996.
- Attema, E.P.W., and F.T. Ulaby, Vegetation modeled as a water cloud, *Radio Sci.*, 13(2), 357-364, 1978.
- Autret, M., R. Bernard, and D. Vidal-Madjar, Theoretical study of the sensitivity of the microwave backscattering coefficient to the soil surface parameters. *Int. J. Remote Sens.* 10(1), 171-179, 1989.
- Beaudoin, A., M. Deshayes, L. Piet, N. Stussi, and T. Le Toan, Retrieval and analysis of temperate forest backscatter signatures from multitemporal ERS-1 data over hilly terrain, 1st Symp. ERS-1 Pilot Project, Toledo, Spain, 23-25 June 1994, 283-289, 1994.
- Benallegue, M., N. Normand, S. Galle, M. Dechambre, D. Taconet, D. Vidal-Madjar, and L. Prevot, Soil moisture assessment at a basin scale using active microwave remote sensing: the AGRISCATT'88 airborne campaign on the Orgeval watershed, *Int. J. Remote Sens.*, 15(3), 645-656, 1994.
- Bernard, R., P. Martin, J. Thony, M. Vauclin, and D. Vidal-Madjar, C-band radar for determining surface soil moisture, *Remote Sens. Environ.*, 12, 189-200, 1982.
- Bertuzzi, P., A. Chanzy, D. Vidal-Madjar, and M. Autret, The use of a microwave backscatter model for retrieving soil moisture over bare soil. *Int. J. Remote Sens.*, 13(14), 2653-2668, 1992.
- Blake, G.R., and K.H. Hartge, Bulk density. In: *Methods of soil analysis. Part 1 - Physical and mineralogical methods* (Klute, A., ed.). ASA/SSA, Madison, WN, 1986, Chap. 13, pp. 363-375, 2nd ed.
- Bouman, B.A.M., Crop parameter estimation from ground-based X-band (3 cm wave) radar

- backscattering data, *Remote Sens. Envir.*, 37, 193-205, 1991.
- Breckenfeld, D.H., Soil survey of Walnut Gulch Experimental Watershed, Arizona, Soil Conservation Service, USDA, 1993, 130 pp.
- Brisco, B., D.J. Major, and M.J. Brown, Multi-parameter radar backscatter of soil moisture from bare and crop covered fields (preliminary results). *Proceedings of 14th Canadian Symp. Remote Sens.*, Calgary, Alberta, Canada, pp. 520-525, 1991.
- Bruckler, L., H. Wittono, and P. Stengel, Near surface soil moisture estimation from microwave measurements. *Remote Sens. Environ.* 26, 101-121, 1988.
- Bruniquel, J., *Contributions de donnees multi-temporelles a l'amelioration radiometriques et a l'utilisation d'images de radar a synthese d'ouverture*, Universite Paul Sabatier, Toulouse, France, 1996 (Ph.D. thesis).
- Canfield, R.H., Application of the line-intercept method in sampling range vegetation, *J. For.*, 39, 388-394, 1941.
- Cognard, A.L., C. Loumagne, M. Normand, P. Olivier, C. Otte, D. Vidal-Madjar, S. Louahala, and A. Vidal, Evaluation of the ERS1/synthetic aperture radar capacity to estimate surface soil moisture: two-year results over the Naizin watershed, *Water Resour. Res.*, 31(4), 975-982, 1995.
- Dobson, M.C., and F.T. Ulaby, Microwave backscatter dependence on surface roughness, soil moisture and soil texture: Part III - soil tension, *IEEE Trans. Geosci. Remote Sens.*, 19, 51-61, 1981.
- Engman, E.T., and N. Chauhan, Status of microwave soil moisture measurements with remote sensing, *Remote Sens. Environ.*, 51, 189-198, 1995.
- Gelderman, F.W., *Soil survey of Walnut Gulch experimental watershed, Arizona*, report, Soil Conserv. Serv. and Agric. Res. Serv., USDA, 1970.

- Houser, P.R., *Remote sensing of soil moisture using four dimensional data assimilation*, University of Arizona, Tucson, AZ, 1996. (Ph.D. dissertation).
- Jackson, T.J., and T.J. Schmugge, Vegetation effects on the microwave emission of soils, *Remote Sens. Envir.*, 36, 203-212, 1991.
- Jackson, T.J., and P. O'Neill, Aircraft scatterometer observations of soil moisture on rangeland watersheds, *Int. J. Remote Sens.*, 6, 1135-1152, 1985.
- John, B., Soil moisture detection with airborne passive and active microwave sensors. *Int. J. Remote Sens.*, 13(3), 481-491, 1992.
- Kline, P., *An easy guide to factor analysis*, Routledge, New York, NY, 1994, 194 pp.
- Kustas, W.P., and D.C. Goodrich, Preface, *Water Resour. Res.*, 30(5), 1211-1225, 1994.
- Mo, T., T. Schmugge, and T.J. Jackson, Calculations of radar backscattering coefficient of vegetation-covered soils, *Remote Sens. Environ.*, 15, 119-133, 1984.
- Moran, M.S., T.R. Clarke, W.P. Kustas, M. Wertz, and S.A. Amer, Evaluation of hydrologic parameters in a semiarid rangeland using remotely sensed spectral data, *Water Resour. Res.*, 30(5), 1287-1297, 1994.
- Moran, M.S., A.F. Rahman, J.C. Washburne, D.C. Goodrich, M.A. Wertz, and W.P. Kustas, Combining the Penman-Monteith equation with measurements of surface temperature and reflectance to estimate evaporation rates of semiarid grassland, *Agr. For. Meteor.*, 80, 87-109, 1996.
- Prevot, L., I. Champion, and G. Guyot, Estimating surface soil moisture and leaf area index of a wheat canopy using a dual-frequency (C and X bands) scatterometer, *Remote Sens. Environ.*, 46, 331-339, 1993a.

- Prevot, L., M. Dechambre, O. Taconet, D. Vidal-Madjar, and S. Galle, Estimating the characteristics of vegetation canopies with airborne radar measurements, *Int. J. Remote Sens.*, 14, 2803-2819, 1993b.
- Rao, R.G.S., and F.T. Ulaby, Optimal spatial sampling techniques for ground truth data in microwave remote sensing of soil moisture, *Remote Sens. Environ.*, 6, 289-301, 1977.
- Rao, K.J., S. Raju, and J.R. Wang, Estimation of soil moisture and surface roughness parameters from backscattering coefficient. *IEEE Trans. Geosci. Remote Sens.* 31(5), 1094-1099, 1993.
- Schmugge, T.J., Remote sensing of soil moisture: recent advances. *IEEE Trans. Geosci. Remote Sens.*, 21(3), 336-344, 1983.
- Schmugge, T., *Remote sensing of soil moisture*, in: Hydrological Forecasting (M.G. Anderson and T.P. Burt, eds.), John Wiley & Sons, New York, Chap. 5, pp. 101-124, 1985.
- Schmullius, C. and R. Furrer, Frequency dependence of radar backscattering under different moisture conditions of vegetation-covered soil, *Int. J. Remote Sens.*, 13(12), 2233-2245, 1992a.
- Schmullius, C., and R. Furrer, Some critical remarks on the use of C-band radar data for soil moisture detection, *Int. J. Remote Sens.*, 13(17), 3387-3390, 1992b.
- Simanton, J.R., R.M. Dixon, and I. McGowan, A microroughness meter for evaluating rainwater infiltration, Proceedings of Hydrology and Water Resources in Arizona and the Southwest, Flagstaff, AZ, April 14-15, 8, 171-174, 1978.
- Taconet, O., D. Vidal-Madjar, C. Emblanch, and M. Normand, Taking into account vegetation effects to estimate soil moisture from C-band radar measurements, *Remote Sens. Environ.*, 56, 52-56, 1996.
- Troufleau, D., A. Vidal, A. Beaudoin, M.S. Moran, M.A. Weltz, D.C. Goodrich, J.

Washburn, and A.F. Rahman, Using optical-microwave synergy for estimating surface energy fluxes over semi-arid rangeland, Proceedings of VI Int. Symp. on Physical Measurements and Signatures on Remote Sensing, 17-21 Jan., Vald'Isere, France, 1994.

Ulaby, F.T., and P.P. Batlivala, Optimum radar parameters for mapping soil moisture, *IEEE Trans. Geosci. Electronics*, 14(2), 81-93, 1976.

Ulaby, F.T., P.P. Batlivala, and M.C. Dobson, Microwave backscatter dependence on surface roughness, soil moisture, and soil texture. Part I - bare soil, *IEEE Trans. Geosci. Electronics*, 16(4), 286-295, 1978.

Ulaby, F.T., G.A. Bradley, and M.C. Dobson, Microwave backscatter dependence on surface roughness, soil moisture, and soil texture: Part II - vegetation-covered soil, *IEEE Trans. Geosci. Electronics*, 17(2), 33-40, 1979.

Ulaby, F.T., R.K. Moore, and A.K. Fung, Microwave remote sensing: active and passive, v. III, Artec House, Dedham, MA., 1986.

Warrick, A.W., S.A. Musil, and J.F. Artiola, *Statistics in pollution science*. In: Pollution Science, Pepper, I.L., C.P. Gerba, and M.L. Brusseau (eds.), San Diego, Academic Press, 1996, Chap. 8, pp. 95-114.

Wei, M.Y., *Soil moisture*. Report of a Workshop held in Tiburon, California, 25-27 Jan., 1994, NASA, 77 pp. , 1995 (NASA CP-3319).

Table 1. Description of Physical Characteristics of the Elgin-Stronghold and Luckyhills-McNeal Soil Units.

Parameters	Elgin-Stronghold Complex	Luckyhills-McNeal Complex
Soil Classification	Paleargid (Elgin) Calciorthid (Stronghold)	Calciorthid (Luckyhills) Haplargid (McNeal)
Slope	8 - 15%	3 - 8 %
Landform	Fan terraces	Fan terraces
Soil Color	Dark brown (0-2.5 cm)	Pale brown (Luckyhills, 0-5 cm) Strong brown (McNeal, 0-2.5 cm)
Texture	Very gravelly sandy loam (0-2.5 cm)	Very gravelly sandy loam (0-2.5 cm)

[from Breckenfeld, 1993]

Table 2. Synthetic Aperture Radar and Field Data for Grass-Dominated Sites.

Sampling Point	UTM ^a (East-West)	UTM (North-South)	Soil Series	Backscattering Coefficient (dB)	
				DOY 206 ^b	DOY 116 ^c
1	3510114	594807	Stronghold	-9.62	-10.06
2	3509502	593841	Elgin	-9.76	-10.21
3	3509299	593712	Stronghold	-9.70	-10.67
4	3509169	593339	Stronghold	-10.07	-10.66
5	3513632	593886		-9.14	-10.18
6	3513164	594205	Stronghold	-9.48	-8.85
7	3513343	594762	Stronghold	-9.07	-8.99
8	3512910	595573	Stronghold	-8.64	-8.77
9	3511418	599037	Stronghold	-8.76	-10.53
10	3511174	599609	Stronghold	-9.50	-9.73
11	3511438	599982	Elgin	-9.66	-10.15
12	3511473	600226	Elgin	-9.45	-10.13
13	3510801	600186	Elgin	-9.66	-10.31
14	3510637	599997	Stronghold	-9.34	-9.26
15	3510846	600609	Elgin	-8.51	-9.36
16	3511114	601225	Elgin	-7.82	-9.53
17	3511313	601499	Elgin	-8.24	-8.73
18	3511438	601399	Stronghold	-9.19	-9.21
19	3511299	601718	Stronghold	-8.33	-9.07
20	3512114	599395	Stronghold	-9.92	-10.85
21	3512174	599743	Elgin	-8.95	-10.21
22	3512433	601325	Elgin	-9.16	-10.3
23	3512861	599166	Stronghold	-8.88	-9.31
24	3513234	599708	Stronghold	-8.98	-9.75
25	3513483	599305	Stronghold	-9.92	-10.08
26	3513453	599982	Stronghold	-9.63	-8.56

^a Universal Transverse Mercator^b Day of Year in 1994^c Day of Year in 1992

Table 2. - *Continued*

Soil Moisture (g/g)	Bulk Density (g/cm ³)	RMS height (cm)	Biomass (g/m ²)	Surface Rock Fragment (%)	Slope (%)	0 -5 cm Depth		
						% Gravel	% Clay	% Sand
9.25 (0.03) ^d	1.51 (0.07)	0.92 (0.29)	384	33				
6.43 (0.30)	1.70 (0.03)	0.77 (0.37)	165	35	9	27	17	55
9.59 (0.26)	1.72 (0.06)	0.85 (0.41)			5	22	17	65
7.78 (0.11)	1.70 (0.09)	0.81 (0.47)			10	33	16	62
4.91 (0.19)	1.58 (0.11)	0.92 (0.36)	762	26				
6.65 (0.08)	1.51 (0.04)	1.73 (0.50)	510	29	6	15	14	56
5.09 (0.15)	1.64 (0.04)	1.48 (0.37)			7	48	15	58
7.16 (0.18)	1.54 (0.07)	1.53 (0.33)	220	34	4	37	14	60
8.07	1.63 (0.09)	0.67 (0.19)	390	30	7	25	17	60
8.28	1.57 (0.05)	1.16 (0.88)	336	28	10	28	18	60
3.00	1.66 (0.03)	0.79 (0.42)			9	20	20	60
1.76	1.50 (0.13)	0.74 (0.39)			12	46	13	65
4.72	1.62 (0.01)	0.89 (0.58)			12	38	27	58
6.74	1.81 (0.13)	1.43 (0.40)			7	26	15	63
2.57	1.54 (0.08)	1.64 (0.59)			12	36	18	60
3.64	1.43 (0.07)	1.30 (0.56)			10	35	18	65
3.52	1.75 (0.04)	1.58 (0.37)	185	22	7	25	18	60
1.80	1.41 (0.03)	1.12 (0.45)			15	20	12	67
2.33	1.50 (0.10)	1.82 (0.42)			13	18	15	60
3.31	1.31 (0.01)	0.68 (0.27)			15	30	18	62
2.46	1.38 (0.14)	1.15 (0.49)			5	15	39	36
3.36	1.44 (0.04)	0.83 (0.29)			10	46	28	56
1.70	1.48 (0.10)	1.08 (0.40)			15	39	15	57
1.13	1.57 (0.14)	1.16 (0.40)			15	46	12	60
1.00	1.35 (0.11)	0.92 (0.44)	189	33	15	36	15	59
1.82	1.44 (0.06)	1.99 (0.60)	269	33	12	34	15	65

^d Bracket Numbers Represent Coefficient of Variation

Table 3. Synthetic Aperture Radar and Field Data for Shrub-Dominated Sites.

Sampling Point	UTM ^a (East-West)	UTM (North-South)	Soil Series	Backscattering Coefficient (dB)	
				DOY 206 ^b	DOY 116 ^c
1	3512550	585919	Luckyhills	-9.39	-9.79
2	3511915	586178	Luckyhills	-8.56	-9.54
3	3511214	586882	Luckyhills	-8.67	-9.03
4	3509980	586177	Luckyhills	-9.18	-10.34
5	3510284	585769	Luckyhills	-8.29	-8.78
6	3505697	593802		-9.99	-10.82
7	3506746	594404		-8.97	-8.9
8	3507806	593359		-8.99	-10.07
9	3507567	592558		-8.19	-9.09
10	3511154	588333	Luckyhills	-7.86	-8.61
11	3513025	588458	Luckyhills	-7.92	-9.90
12	3512517	588488		-8.11	-9.33
13	3512751	589841	McNeal	-7.78	-9.62
14	3511811	589109	Luckyhills	-8.73	-9.33
15	3512092	589711		-9.47	-9.85
16	3511383	589706	Luckyhills	-8.88	-9.74
17	3511000	589044	Luckyhills	-9.29	-8.61
18	3512040	590393	Luckyhills	-9.61	-9.69
19	3511716	590388	Luckyhills	-8.49	-8.18
20	3510398	592299		-10.08	-11.34
21	3508993	592309		-9.00	-9.87

^a Universal Transverse Mercator^b Day of Year in 1994^c Day of Year in 1992

Table 3. - *Continued*

Soil Moisture (g/g)	Bulk Density (g/cm ³)	RMS height (cm)	Biomass (g/m ²)	% Surface Rock Fragment	0 - 5 cm Depth			
					% Slope	% Gravel	% Clay	% Sand
5.42 (0.15) ^d	1.50 (0.05)	0.82 (0.46)			6	29	16	60
6.22 (0.16)	1.54 (0.01)	1.14 (0.51)	286	52	5	16	11	77
5.49 (0.11)	1.41 (0.02)	1.36 (0.31)			3	45	16	60
2.75 (0.28)	1.43 (0.14)	0.80 (0.35)			3	25	24	53
3.98 (0.20)	1.57 (0.03)	1.52 (0.47)	344	37	4	55	14	63
6.29 (0.41)	1.59 (0.00)	0.72 (0.55)	329	49				
5.34 (0.10)	1.50 (0.13)	1.45 (0.42)	627	37				
3.58 (0.35)	1.51 (0.06)	0.81 (0.64)						
5.34 (0.05)	1.48 (0.05)	1.32 (0.53)						
6.12 (0.08)	1.52 (0.14)	1.49 (0.29)			5	26	13	65
11.74 (0.14)	1.60 (0.08)	0.92 (0.74)			4	24	16	62
10.46 (0.29)	1.52 (0.07)	1.17 (0.33)	543	38				
8.30 (0.13)	1.82 (0.13)	0.94 (0.59)			5	55	16	58
6.90 (0.03)	1.68 (0.09)	0.96 (0.47)			4	28	15	60
7.78 (0.12)	1.50 (0.03)	0.90 (0.39)						
5.66 (0.06)	1.68 (0.14)	0.97 (0.42)	415	27	8	23	10	83
7.88 (0.10)	1.47 (0.10)	1.34 (0.38)				26	15	70
7.06 (0.05)	1.58 (0.07)	0.91 (0.39)	415	35	8	35	16	55
6.25 (0.11)	1.49 (0.12)	1.42 (0.32)			10		10	73
6.67 (0.10)	1.64 (0.09)	0.64 (0.29)						
4.60 (0.06)	1.69 (0.07)	1.00 (0.45)	450	42				

^d Bracket Numbers Represent Coefficient of Variation

Table 4. Partial Correlation Coefficients Between Radar Backscattering Coefficient and Volumetric Soil Moisture Content for Grass-dominated and Shrub-dominated Sites.

	Backscattering Coefficient (dB)	Soil Moisture (%)	RMS height (cm)
<i>Grass-dominated Sites</i>			
Backscattering Coefficient (dB)	1.00		
Soil Moisture (%)	-0.18	1.00	
RMS height (cm)	0.45	-0.08	1.00
<i>Shrub-dominated Sites</i>			
Backscattering Coefficient (dB)	1.00		
Soil Moisture (%)	0.46	1.00	
RMS height (cm)	0.64	-0.39	1.00

Table 5. Coefficients of Variation and Number of Samples Required to Obtain 10 % Accuracy of Soil Moisture Content for Three Sites with Different Slopes (Interval of Confidence = 99 %).

Site	Coefficient of Variation	Number of Samples
Flat	0.15	60
North-faced slope	0.17	77
Hilly-shaped slope	0.27	193

FIGURE CAPTIONS

- Figure 1. Map of the Walnut Gulch Experimental Watershed showing its geographical location in the State of Arizona.
- Figure 2. Walnut Gulch Experimental Watershed boundaries with location of soil moisture sampling sites.
- Figure 3. Scatterplot between 1992 dry season SAR image and 1994 wet season SAR image for (a) grass-dominated and (b) shrub-dominated sites. Numbers above the symbols represent the sampling sites.
- Figure 4. Scatterplot between 1992 dry season SAR image and soil roughness data for (a) grass-dominated and (b) shrub-dominated sites.
- Figure 5. Scatterplots between % volumetric soil moisture content and (a) wet season backscattering coefficients, grass-dominated sites; (b) difference (wet - dry) backscattering coefficients, grass-dominated sites; (c) wet season backscattering coefficients, shrub-dominated sites; and (d) difference (wet - dry) backscattering coefficients, shrub-dominated sites. Numbers above the symbols represent the site identifications. The dashed lines correspond to the confidence interval of the linear regression at 95%. *S.E.* = standard error; *n* = number of samples.

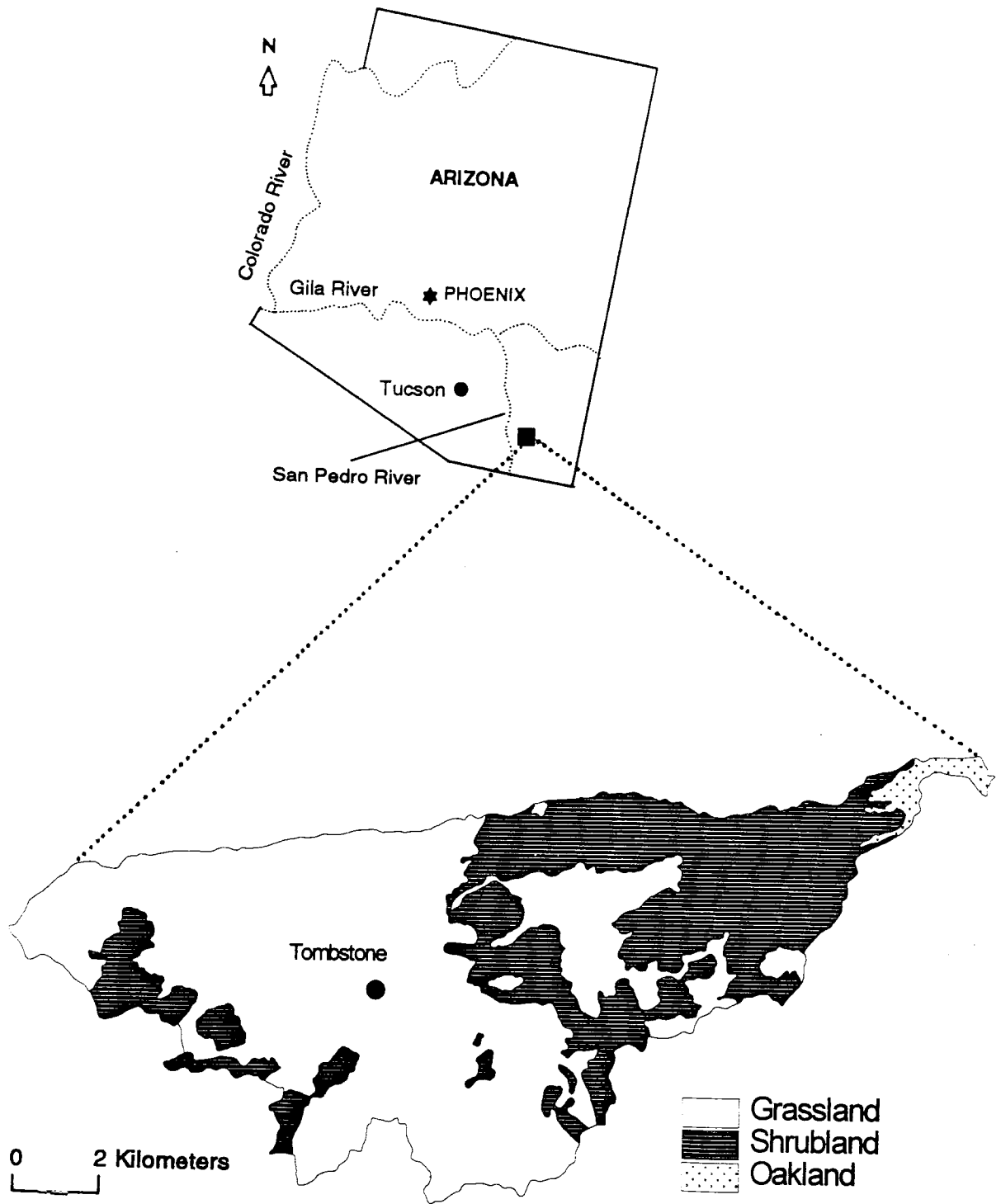


Figure 1

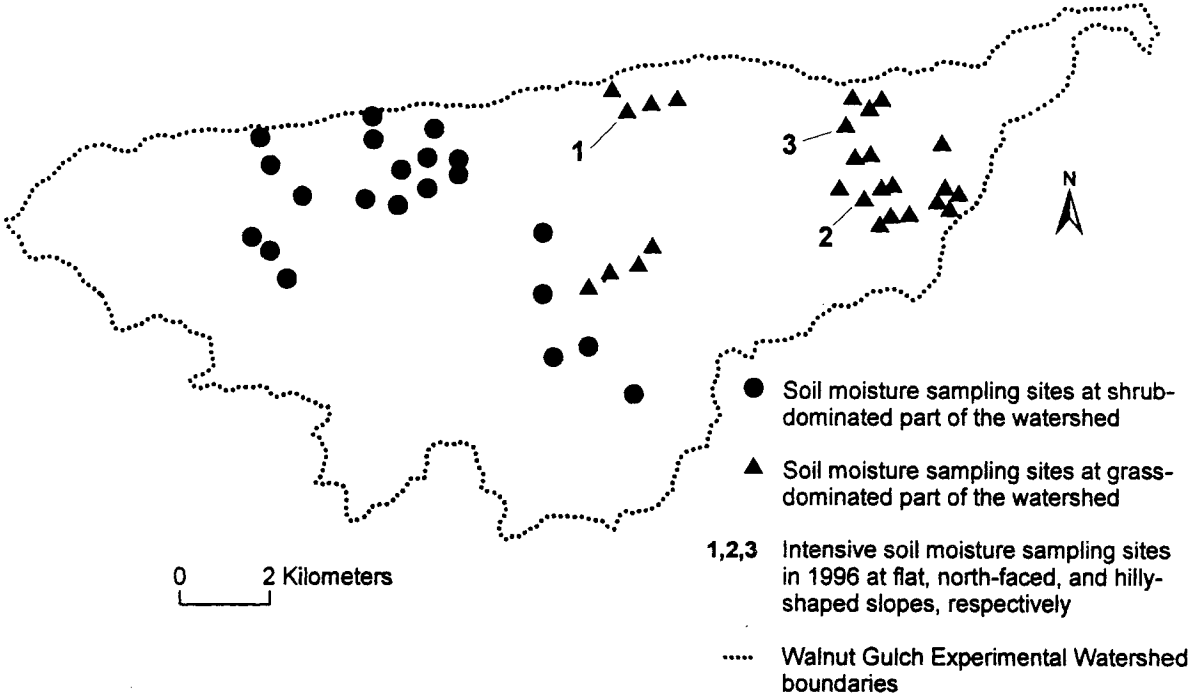


Figure 2

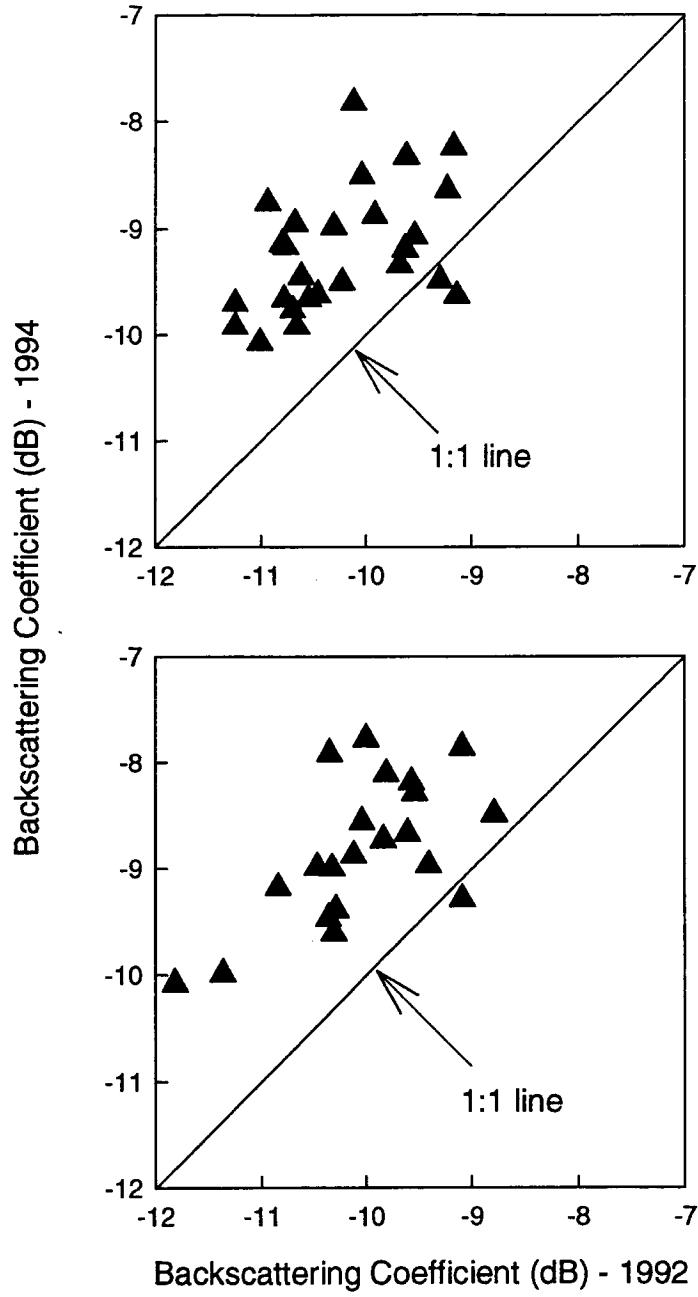


Figure 3

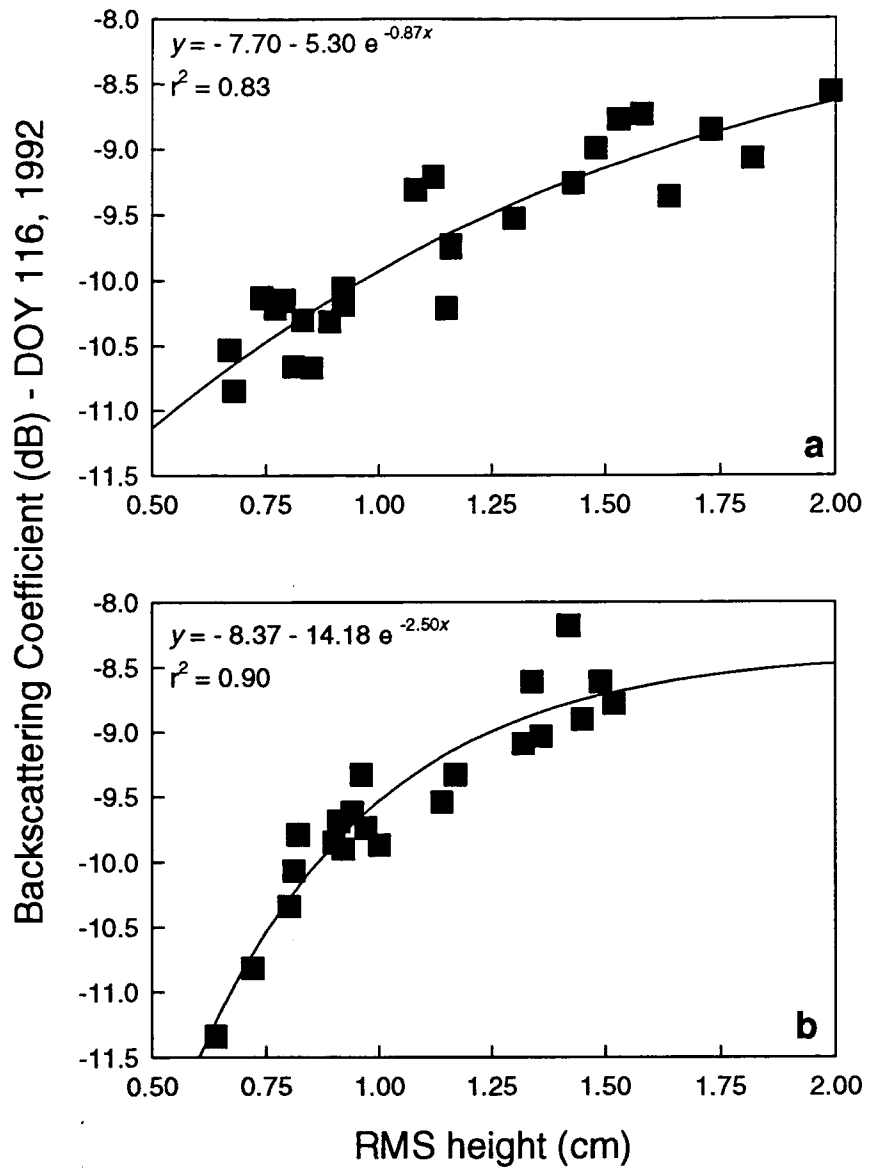
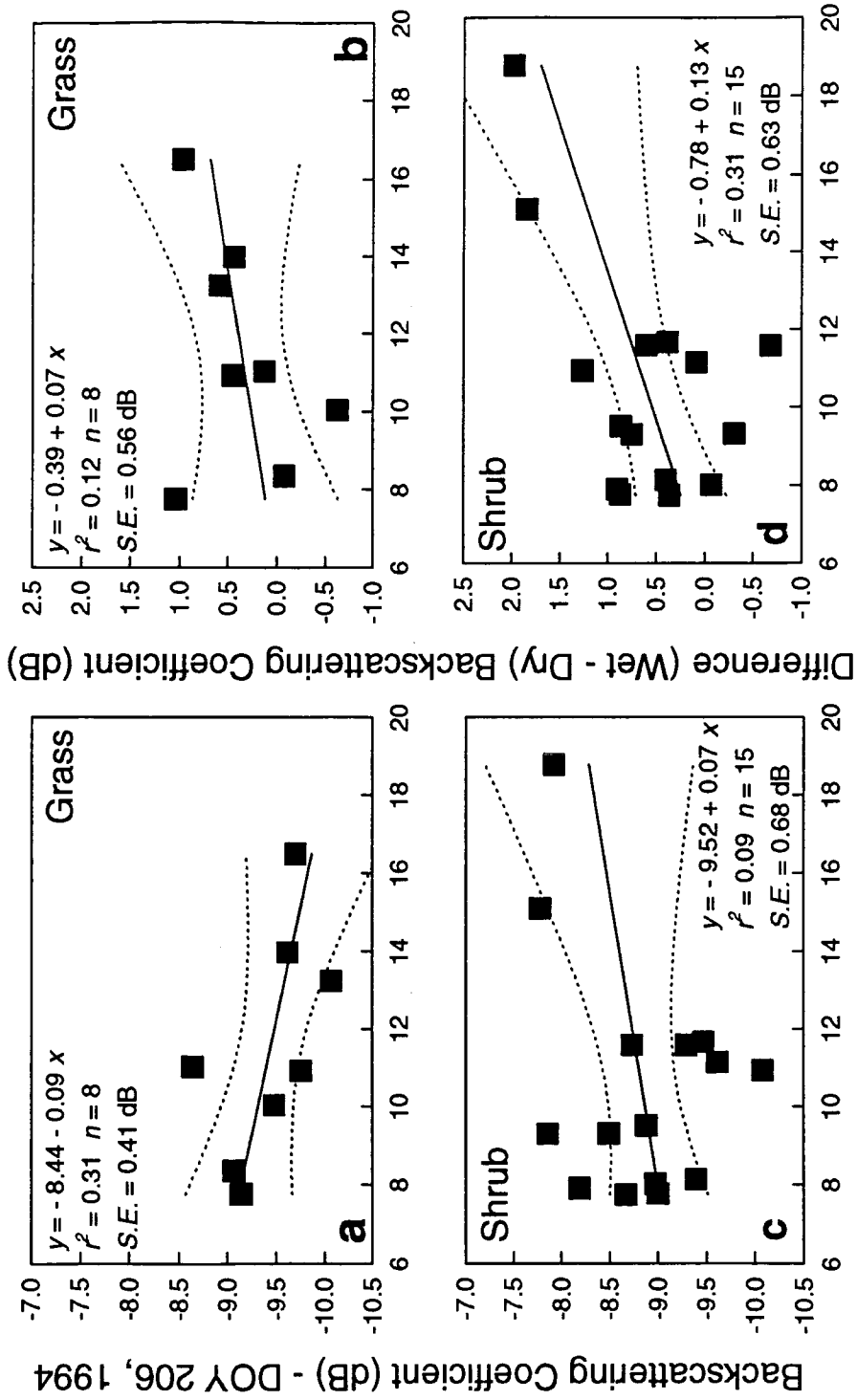


Figure 4



% Volumetric Soil Moisture

Figure 5

APPENDIX B:

The Use of Microwave and Optical Synergism for Estimation of Soil Moisture Content from C-band Synthetic Aperture Radar Data in a Semi-Arid RangelandE. E. Sano¹, J. Qi², and A. R. Huete¹

¹ Department of Soil, Water and Environmental Science, The University of Arizona, 429 Shantz Bldg # 38, Tucson, AZ, 85721, USA

² USDA-SWRC, 2000 E. Allen Road, Tucson, AZ, 85719, USA

to be submitted to "IEEE Transactions on Geoscience and Remote Sensing"

ABSTRACT

Estimation of soil moisture from C-band synthetic aperture radar (SAR) systems operating at single polarization and single incidence angle is often difficult because of the influence of vegetation and soil roughness. To improve soil moisture estimates in a semiarid region from such a system configuration, SAR data from the European Remote Sensing Satellite (ERS-1) were combined with the Landsat Thematic Mapper (TM) data. The SAR data were compared with soil moisture measurements at three different conditions: a) without any correction for soil roughness and vegetation effects; b) partially corrected for soil roughness effects; and c) fully corrected for soil roughness and vegetation effects. The soil roughness influence was taken into account by using the difference ($\sigma^\circ - \sigma^\circ_{\text{dry}}$), where σ° and $\sigma^\circ_{\text{dry}}$ refer to the backscattering coefficient σ° from a given image and from a dry season SAR image, respectively. The vegetation influence was corrected by using an empirical relationship between σ° and leaf area index, the latter being derived from TM images. Results indicated that the contribution of soil roughness and vegetation in the radar backscatter in a semiarid region were significant and they must be minimized to improve the accuracy of soil moisture estimation using C-band.

INTRODUCTION

A number of investigations have shown the potential of active microwave remote sensing to retrieve surface soil moisture content [1] - [4]. This is possible because of a large contrast between the dielectric constant ϵ of liquid water (~ 80) and dry soil (3-5) [5]. For

instance, the dielectric constant of a sandy loam soil can increase from 5 to more than 20 when volumetric soil moisture varies from 0 to 20 % [6].

Studies from late 1970s and early 1980s [1], [2], [7] reported that the C-band (5.3 GHz) with an incidence angle around 10° was the optimum configuration for soil moisture retrieval. However, current spacecraft platforms acquire images at larger angles to obtain a high range of spatial resolutions (magnitude of tens of meters) [8], [9]: 23° for the European Remote Sensing (ERS-1 and ERS-2) satellites, and 38° for the Japanese Earth Resources Satellite (JERS-1). The exception is the Canadian Remote Sensing Satellite (RADARSAT), which operates at a range of 10°-60°. At this range of incidence angles, the effects of vegetation and roughness on the radar backscattering process can not be neglected [10], [11].

The effects of vegetation can be reduced by using a first-order, semi-empirical backscatter model known as 'water cloud' [12]. The model computes the radar backscattering coefficient σ^o of a canopy as the sum of the contributions of the vegetation layer and the soil, the latter attenuated through the vegetation:

$$\sigma^o = \sigma_{\text{veg}}^o + \tau^2 \sigma_{\text{soil}}^o \quad (\text{unit: m}^2/\text{m}^2) \quad (1)$$

where σ_{veg}^o is the scattering contribution from the vegetation volume (unit: m^2/m^2), τ^2 is the two-way attenuation of the SAR signal from the vegetation layer, and σ_{soil}^o is the scattering contribution from the soil underneath (units = decibels, dB). The parameters σ_{veg}^o , σ_{soil}^o , and τ^2 are expressed as follows [13]:

$$\sigma_{\text{veg}}^{\circ} = AV_1 \cos \theta (1 - \tau^2) \quad (\text{unit: m}^2/\text{m}^2) \quad (2)$$

$$\sigma_{\text{soil}}^{\circ} = C + D h_v \quad (\text{units: dB}) \quad (3)$$

$$\tau^2 = \exp(-2BV_2 / \cos \theta) \quad (4)$$

where A , B , V_1 , and V_2 are parameters related to the canopy type; C is a roughness dependent parameter; D is a constant that depends upon the sensor configuration; θ is the sensor incidence angle relative to nadir; and h_v is the volumetric soil moisture content.

The radar backscatter signal at high frequencies is particularly sensitive to vegetation [13], [14], whereas at low frequencies is particularly sensitive to soil moisture [3], [9], [15]. Thus, a combination of high- and low-frequency SAR data over agricultural sites has been used to improve the estimation of soil moisture [16] - [19]. In these cases, the vegetation-induced attenuation (τ^2) was determined by using a low-frequency SAR data. These studies also demonstrated that the term $\sigma_{\text{veg}}^{\circ}$ for low-frequency SAR data was important only when vegetation density is high. In sparsely vegetated areas, the contribution from vegetation in the scattering process is assumed to be significantly smaller than the contribution from soil ($\sigma_{\text{veg}}^{\circ} \ll \sigma_{\text{soil}}^{\circ}$) so that the term $\sigma_{\text{veg}}^{\circ}$ can be neglected.

However, this multifrequency approach can sometimes result in poor soil moisture estimates because both high- and low-frequency SAR data can also be sensitive to soil roughness (parameter C , Eq. 4) [8], [20], [21]. The water cloud model is also difficult to apply in natural ecosystems because the canopy parameters A , B , V_1 and V_2 (see Eqs. 2 and 3) are usually unknown. Furthermore, in arid and semiarid regions, soil moisture contents hardly exceed 20 %, indicating that the contribution from $\sigma_{\text{soil}}^{\circ}$ may be small or approximately

of the same magnitude as σ_{veg}° ($\sigma_{veg}^{\circ} \sim \sigma_{soil}^{\circ}$). Thus, σ_{veg}° may not be neglected.

To account for roughness effects in SAR data, one approach is to use the co-polarized ratio technique, a ratio between HH and VV polarized waves. Although some studies [8], [19] have demonstrated that this technique can significantly reduce soil roughness effects, multipolarization data are unavailable on current satellite-based SAR systems.

Therefore, the techniques to correct for the effects of roughness and vegetation in the radar backscatter for improved soil moisture estimations are limited either to agricultural sites or to a specific sensor configuration. A more practical approach for natural ecosystems, using currently available satellite-based data, needs to be developed. For instance, vegetation effects in SAR data can be accounted for by estimating the vegetation density of the study area via computation of optical-based vegetation indices such as the Normalized Difference Vegetation Index (NDVI) [23]. The NDVI can be related to canopy parameters such as leaf area index (LAI) [24], which can also be related to microwave backscattering coefficients σ° [20]. Thus, the development of an empirical LAI- σ° relationship may be useful to correct the SAR data for vegetation effects.

The objectives of this study were to: a) investigate the effects of vegetation on radar backscatter in a semiarid region; b) investigate the potential of SAR and TM synergism to reduce the vegetation effects in soil moisture retrievals; and c) develop a practical approach to account for soil roughness and vegetation effects in the C-band SAR data to improve the estimation of soil moisture content.

THE EXPERIMENT

Site Description

The study area is located at the Walnut Gulch Experimental Watershed (31.72° N, 110.00° W), a representative site of shrub- and grass-dominated rangelands found in the southwestern part of the United States (Figure 1). The watershed is operated by the U.S. Department of Agriculture (USDA) Agricultural Research Service (ARS) since 1954. The annual precipitation varies from 250 to 500 mm, with approximately two thirds occurring as high intensity thunderstorms with limited areal extent during the summer 'monsoon' season (July and August). The predominant surface soil textures (upper 5 cm) are gravelly loamy sands and sandy loams, with small amounts of organic matter and an average of ~ 30% of surface rock fraction [25] - [27]. The vegetation is a mixture of desert grass and shrubs.

ERS-1 SAR Data

Seven SAR images were acquired in 1992 as part of the WG'92 experiment [28] during the pre-monsoon, monsoon, and post-monsoon seasons and another single image was obtained in 1994 during the wet season (Table 1). The ERS-1 SAR sensor operates at C-band (5.3 GHz) with a 23° incidence angle, resulting in a swath of 100 km at a nominal spatial resolution of 30 m.

The SAR images obtained from the European Space Agency (ESA) were the standard Precision Image products, which had been corrected for antenna elevation, gain pattern, and range spreading loss [10]. These images were georeferenced to the Universal Transverse

Mercator coordinate system (Zone 12, 1927 North American Datum, Clarke 1866), and corrected for topographic effects by accounting for the real backscatter area of each pixel using a digital elevation model [29]. The elevation model was derived from topographic maps in 1:24,000 scale with a contour interval of 6.1 m. Radar backscattering coefficients (σ°) were extracted from these preprocessed images using the following equation :

$$\sigma^{\circ} = 10 \log \left[(\overline{DN}^2 + STD^2) / K \right] \quad (\text{units :dB}) \quad (5)$$

where DN = digital numbers of the site (at least 50 pixels per site);

STD = standard deviation; and

K = calibration constant.

Landsat TM data

Eight Landsat TM scenes were also obtained during the WG'92 experiment and were used in this study (Table 1). The TM sensor operates at six reflective bands located in the visible, near infrared, and middle infrared, and at one thermal band. The optical bands have a nominal spatial resolution of 30 m, while the thermal band has a 120 m spatial resolution. The TM digital numbers were transformed to surface reflectance values in three steps [28], [30], [31]: 1) acquisition of the incident solar illumination data from sunrise to solar noon in the same day of the Landsat overpasses, using a solar radiometer, to account for the atmospheric effects in the TM digital numbers; 2) generation of at-satellite radiance values for a given series of surface reflectance values by using the Herman-Browning radiative

transfer code [31]; and 3) generation of TM reflectance images from values derived from the radiative transfer code and from Landsat TM sensor calibrations. All TM images were also georeferenced to the UTM coordinate system (total RMS error = 1.5 pixel).

Leaf area index (LAI) values were calculated for all Landsat TM scenes by using the following empirical relationship proposed for arid and semiarid regions [24]:

$$\text{LAI} = -0.352 + 6.124 \text{NDVI} - 15.24 \text{NDVI}^2 + 18.99 \text{NDVI}^3 \quad (6)$$

where NDVI is defined as:

$$\text{NDVI} = (\rho_{\text{NIR}} - \rho_{\text{Red}}) / (\rho_{\text{NIR}} + \rho_{\text{Red}}) \quad (7)$$

where ρ_{Red} and ρ_{NIR} are the surface reflectances in red and near infrared spectral regions, respectively.

Soil Moisture Data

Gravimetric samples for soil moisture content were collected at the Meteorological-Energy flux (MF) stations 1, 3, 5 and 6 (six replicates) during the pre-monsoon, monsoon, and post-monsoon seasons of 1992 (Table 1). These six replicates were averaged to one reading. Volumetric soil moisture contents were derived using previously measured bulk densities (1.44 ~ 1.83 g/cm³) [32]. Soil moisture measurements were also made on the same day of the ERS-1 SAR satellite overpass in 1994 at 21 validation sites in the shrub-dominated part of the watershed (three replicates). Dry bulk density data were obtained for each site by the excavation method [33], allowing for the calculation of volumetric soil moisture.

APPROACH

Investigation Sites

The SAR and TM data obtained in 1992 from MF sites 1, 2, 3, 7, and 8 were selected to investigate the use of SAR/TM synergism to correct the effects of vegetation in the SAR data, in order to obtain an improved estimation of soil moisture content from radar data in the watershed. Metflux sites 4, 5, and 6, located in the eastern, grass-dominated side of the watershed, were not included in the analyses because of the limited number of available SAR images. The analysis was performed in four steps. The first step was to verify the relationship between SAR and TM data. This was done by comparing the temporal values of σ° and LAI simultaneously and by analyzing the linear regression equations between these two parameters.

The second step was to correct the radar backscattering coefficients for the effects of the soil roughness. The technique involved a subtraction ($\sigma^\circ - \sigma^\circ_{\text{dry}}$) [34]; that is, the σ° from a given image was subtracted by the σ° from a dry season image. The assumption in this step was that the soil roughness was the only important parameter in the backscattering process during the dry season. The coefficients derived from this subtraction is referred as σ°_1 hereafter.

The third step was to find an empirical relationship between σ°_1 and LAI. This relation corresponds to the linear regression equation obtained by considering all MF sites with coefficients of determination r^2 between σ° and LAI larger than 0.50.

The final step was to correct the vegetation effects on σ°_1 . The residuals of radar

backscattering coefficients for the MF sites were calculated by subtracting the measured and the estimated σ°_1 values. The measured values refer to the backscattered signals obtained from the subtraction of σ° from a dry season image, while the estimated σ°_1 values refer to the backscatter signals calculated from the empirical σ°_1 -LAI relation. The radar backscattering coefficients corrected for both soil roughness and vegetation is referred as σ°_2 hereafter. To verify the performance of this approach, the soil moisture contents obtained in 1992 were compared with the backscattering coefficients at three steps: 1) without any correction; 2) partially corrected for soil roughness effects; and 3) fully corrected for soil roughness and vegetation effects.

Validation Sites

To validate the approach discussed above, an additional 21 sites located in the shrub-dominated sites and in the Luckyhills-McNeal complex soil unit [26] in the watershed were selected [20]. Again, validation sites in the grass-dominated part of the watershed were not included in this study because of the limited number of SAR data. The soil moisture contents measured during the ERS-1 SAR overpass (DOY 206, 1994) from these sites were compared with the radar backscattering coefficients at three steps: 1) without any correction; 2) partially corrected for soil roughness; and 3) fully corrected for soil roughness and vegetation effects. The LAI- σ°_1 relation obtained from the investigation sites (1992 data set) were applied to account for the vegetation effects.

RESULTS

Investigation Sites

The microwave, optical and field data from the Metflux sites are shown in Table 2. Figure 2 shows a temporal pattern (April to November, 1992) of both LAI and σ° at MF sites 1, 2, 3, 7, and 8. Because the ERS-1 and Landsat satellite overpasses were not coincident, LAI values were linearly interpolated at the ERS-1 SAR overpasses by using two adjacent LAI values. The assumption was that the soil drying was uniform and that no rain occurred during the two TM overpasses. We can notice a good degree of similarity between LAI and σ° , particularly from DOY 160 to DOY 290. The only exception was the trend for MF 3, where the backscattering coefficient remained approximately constant from DOY 114 to DOY 306, 1992. The year 1992 had a very wet spring [28], which was responsible for the unusually high LAI values for DOY 114. On the other hand, the unusually high σ° values for DOY 310, particularly at MF stations 1, 2 and 7, were probably due to a high soil moisture content at these sites.

Figure 3 shows the scatterplot between LAI and radar backscattering coefficients for the SAR data on DOYs 135, 170, 240, 275, and 291. We can notice good linear relationships between LAI and σ° at MF 1, 2 and 7 ($r^2 = 0.98, 0.55, \text{ and } 0.83$, respectively; confidence interval of 95%). These three sites were used to derive the empirical LAI and σ° relation for the MF sites (Figure 4).

Figure 5a shows a scatterplot between percent volumetric soil moisture content versus radar backscattering coefficients σ° for MF sites 1 and 3, for four different dates. These MF

sites were the only two sites where all SAR, TM, and soil moisture data were available. Soil moisture data from MF site 3 were not available for DOYs 274 and 290. Despite a low range of soil moisture contents (less than 3%), we can notice a high variation in σ° (from -12 to -8.5 dB, approximately) at MF1. Assuming that soil roughness did not change over the time period analyzed in this study and considering the low soil moisture conditions for all four SAR overpasses, we can conclude that this large variation in σ° was due to changes in vegetation conditions. Thus, we can expect all MF1 points in the Figure 5a to be close each other after removing the effects of vegetation.

To remove soil roughness effects, we subtracted all multitemporal σ° values from the DOY 170 σ° , since the lowest backscattering coefficients for all MF sites were found on this date. Figure 5b shows a scatterplot between percent volumetric soil moisture content and radar backscatter corrected for soil roughness influences (σ_1°), for MF1 and MF3. We can notice that the DOY 130 σ_1° of MF3, which was higher than that from MF1 in Figure 5a, is now lower than that for MF1. This tendency suggests that the soil roughness effects was higher for MF3 than for MF1.

Figure 5c shows the scatterplot between soil moisture and radar backscattering coefficients (σ_2°) of MF sites 1 and 3, corrected for soil roughness and vegetation influences. All four data points of MF1 are now closer to each other because the soil moisture contents were similar for all dates. For MF3, the range of σ_2° variation remained approximately the same between DOYs 130 and 162, even after correcting for roughness and vegetation effects. The relatively small variation of σ° for this site in comparison to the other MF sites over the

entire period of the WG'92 experiment (Figure 2) was the main reason for this particular trend.

Validation Sites

The SAR and field data from 21 investigation sites in the shrub-dominated part of the watershed is shown in Table 3, while Table 4 shows the r^2 values between LAI and σ^0 for these sites. The LAI values were derived from 1992 TM data and interpolated for the following 1992 SAR overpasses: DOYs 135, 170, 240, 275, and 291. The temporal trends of LAI and σ^0 for sites with coefficients of determination (r^2) values higher than 0.50 are shown in Figure 6. As in MF sites, a good relationship between LAI and σ^0 was also shown for these validation sites. Thus, the empirical LAI- σ^0_1 relation obtained from the MF sites was applicable for these validation sites.

Without roughness and vegetation corrections, the correlation between soil moisture and SAR backscattering coefficient was poor (Figure 7a); that is, the low correlation ($r^2 = 0.36$, for a confidence interval of 95%) and the low slope (0.18) was most likely due to the influence of both soil roughness and vegetation in the backscattering process. When only soil roughness is corrected by using the subtraction technique, the soil moisture and SAR backscattering correlation appeared to be worse, as demonstrated in Figure 7b. We can notice reduced r^2 and slope values (0.05 and 0.14, respectively), in comparison with those obtained without correcting for soil roughness effects. The reason is that the vegetation influences at the sites 1 and 2 were probably higher than for the other sites. Thus, although they presented

the lowest soil moisture contents, their σ_1^0 values were relatively high. Consequently, correction for soil roughness without considering vegetation effects may not improve soil moisture estimation in arid and semiarid regions.

When both soil roughness and vegetation effects were corrected for, the soil moisture and SAR backscatter correlation was substantially improved (Figure 7c). The relatively high r^2 and slope values (0.61 and 0.57, respectively) indicate that the techniques used in this study to account for roughness and vegetation effects were successful. However, the correlation is still lower than expected or lower than those obtained from other regions such as in agricultural areas or in temperate regions ($r^2 > 0.80$, e.g., [2], [11]). The reason for this low correlation is the high spatial variability of soil moisture in the study area, which was discussed in details by Sano et al. [34].

CONCLUSIONS

In this study, we used a microwave and optical synergism to improve the soil moisture content estimation using C-band ERS-1 SAR data in a semiarid region. The following were the major findings:

- a) the C-band radar backscattering coefficients were highly, positively correlated with leaf area index derived from Landsat TM data. This indicates that vegetation in semiarid regions does contribute significantly to the radar backscatter observed with SAR systems. This was mainly due to low soil moisture contents in the semiarid regions (< 20%). In other words, the contribution from soil moisture (typically < 20 % volumetric basis) in

the backscattering process in semiarid regions is not significantly higher than that from vegetation, so that the influence of vegetation becomes significant in a multitemporal radar data analysis.

- b) the influence of soil roughness and the vegetation in the ERS-1 SAR configuration were significant and must be corrected when used for soil moisture estimation using C-band SAR data.
- c) the techniques used in this study to account for soil roughness and vegetation effects allowed us to obtain improved soil moisture estimates and, upon validation, may provide an easy way to correct for effects of these two parameters without using multipolarization or multifrequency SAR data.
- d) the σ^0 -LAI relation obtained from the investigation sites (MF sites) performed well for some of the validation sites; nevertheless, future research involving more multitemporal data and more vegetation types needs to be conducted to obtain a more generic relationship.

ACKNOWLEDGMENTS

Special thanks are due to Steve Land of EOSAT Corp., who provided the Landsat TM images at no cost. Dr. Alain Vidal and Denis Troufleau did the SAR image processing at the CEMAGREF/ENGREF, Montpellier, France. We also acknowledge Dr. Susan Moran

for reviewing the manuscript. This research was partially supported by VEGETATION project at the USDA-ARS Water Conservation Laboratory, NASA EOS Program (NASA Ref. Num. NAG-W2425), NASA-EOS Interdisciplinary Research Program in Earth Sciences (NASA-IDP-88-086), and National Science Foundation Grant # BSC-8920851. The assistance and cooperation of personnel at USDA ARS Southwest Watershed Research Center in Tucson and at USDA ARS Tombstone facility were also greatly appreciated.

REFERENCES

- [1] F.T. Ulaby, and P.P. Batlivala, "Optimum radar parameters for mapping soil moisture," *IEEE Trans. Geosci. Electron.*, vol. 14, no. 2, pp. 81-93, 1976.
- [2] R. Bernard, P. Martin, J. Thony, M. Vauclin, and D. Vidal -Madjar, "C-band radar for determining surface soil moisture," *Remote Sensing Environ.*, vol. 12, pp. 189-200, 1982.
- [3] C. Schmullius, and R. Furrer, "Some critical remarks on the use of C-band radar data for soil moisture detection," *Int. J. Remote Sensing*, vol. 13, no. 17, pp. 3387-3390, 1992.
- [4] E.T. Engman, and N. Chauhan, "Status of microwave soil moisture measurements with remote sensing," *Remote Sensing Environ.*, vol. 51, pp. 189-198, 1995.
- [5] F.T. Ulaby, R.K. Moore, and A.K. Fung, *Microwave remote sensing: active and passive*. Dedham:Artec House, vol. III, 1986.
- [6] M.T. Hallikainen, F.T. Ulaby, M.C. Dobson, M.A. El-Rayes, and L.Wu, "Microwave dielectric behavior of wet soils - Part I: empirical models and experimental observations," *IEEE Trans. Geosci. Remote Sensing*, vol. 23, no. 1, pp. 25-34, 1985.

- [7] F.T. Ulaby, G.A. Bradley, and M.C. Dobson, "Microwave backscatter dependence on surface roughness, soil moisture, and soil texture: Part II - vegetation-covered soil," *IEEE Trans. Geosci. Electron.*, vol. 17, no. 2, pp. 33-40, 1979.
- [8] M. Autret, R. Bernard, and D. Vidal-Madjar, "Theoretical study of the sensitivity of the microwave backscattering coefficient to the soil surface parameters," *Int. J. Remote Sensing*, vol. 10, no. 1, pp. 171-179, 1989.
- [9] P. Bertuzzi, A. Chanzy, D. Vidal-Madjar, and M. Autret, "The use of a microwave backscatter model for retrieving soil moisture over bare soil," *Int. J. Remote Sensing*, vol. 13, no. 14, pp. 2653-2668, 1992.
- [10] A.L. Cognard, C. Loumagne, M. Normand, P. Olivier, C. Otle, D. Vidal-Madjar, S. Louahala, and A. Vidal, "Evaluation of the ERS1/synthetic aperture radar capacity to estimate surface soil moisture: two-year results over the Naizin watershed," *Water Resour. Res.*, vol. 31, no. 4, pp. 975-982, 1995.
- [11] O. Taconet, D. Vidal-Madjar, Ch. Emblanch, and M. Normand, "Taking into account vegetation effects to estimate soil moisture from C-band radar measurements," *Remote Sensing Environ.*, vol. 56, pp. 52-56, 1996.
- [12] E.P.W. Attema, and F.T. Ulaby, "Vegetation modeled as a water cloud," *Radio Sci.*, vol. 13, no. 2, pp. 357-364, 1978.
- [13] L. Prevot, I. Champion, and G. Guyot, "Estimating surface soil moisture and leaf area index of a wheat canopy using a dual-frequency (C and X bands) scatterometer," *Remote Sensing Environ.*, vol. 46, pp. 331-339, 1993a.
- [14] B.A.M. Bouman, "Crop parameter estimation from ground-based X-band (3 cm wave) radar backscattering data," *Remote Sensing Environ.*, vol. 37, pp. 193-205. 1991.
- [15] M.M. Benallegue, S. Galle, M. Dechambre, O. Taconet, D. Vidal-Madjar, and L. Prevot, "Soil moisture assessment at a basin scale using active microwave remote sensing: the Agriscatt'88 airborne campaign on the Orgeval watershed," *Int. J. Remote*

Sensing, vol. 15, pp. 645-656, 1994.

- [16] S. Paloscia, P. Pampaloni, L. Chiarantini, P. Coppo, S. Gagliani, and G. Luzi, "Multifrequency passive microwave remote sensing of soil moisture and roughness," *Int. J. Remote Sensing*, vol. 14, pp. 467-483, 1993.
- [17] L. Prevot, M. Dechambre, O. Taconet, D. Vidal-Madjar, and S. Galle, "Estimating the characteristics of vegetation canopies with airborne radar measurements," *Int. J. Remote Sensing*, vol. 14, pp. 2803-2819, 1993b.
- [18] O. Taconet, M. Benallegue, D. Vidal-Madjar, L. Prevot, M. Decambre, and M. Normand, "Estimation of soil and crop parameters for wheat from airborne radar backscattering data in C- and X- bands," *Remote Sensing Environ.*, vol. 50, pp. 287-294, 1994.
- [19] M.S. Moran, A. Vidal, D. Troufleau, Y. Inoue, and T.A. Mitchell, "Ku- and C-band SAR for discriminating agricultural crop and soil conditions", 1997. (submitted to *Remote Sensing Environ.* journal).
- [20] F.T. Ulaby, C.T. Allen, and G. Eger III, "Relating the microwave backscattering coefficient to Leaf Area Index," *Remote Sensing Environ.*, vol. 14, pp. 113-133, 1984.
- [21] B. Brisco, R.J. Brown, B. Snider, G.J. Sofko, J.A. Koehler, and A.G. Wacker, "Tillage effects on the radar backscattering coefficient of grain stubble fields", *Int. J. Remote Sensing*, vol. 12, pp. 2283-2298, 1991.
- [22] K.S. Chen, S.K. Yen, and W.P. Huang, "A simple model for retrieving bare soil moisture from radar-scattering coefficients," *Remote Sensing Environ.*, vol. 54, pp. 121-126, 1995.
- [23] D.W. Deering, *Rangeland reflectance characteristics measured by aircraft and spacecraft sensors*. Ph.D. Dissertation, Texas A & M University, College Station, TX, 1978.

- [24] J. Qi, Y.H. Kerr, M. Weltz, M.S. Moran, and S. Sorooshian, 1997. "A synergistic approach to estimating leaf area index with models and remote sensing data over a semi-arid region", submitted to *Remote Sensing Environ.*
- [25] F.W. Gelderman, *Soil survey of Walnut Gulch experimental watershed, Arizona*, Soil Conservation Service/Agricultural Research Service, USDA, 1970.
- [26] D.H. Breckenfeld, *Soil survey of Walnut Gulch Experimental Watershed, Arizona*, Soil Conservation Service, USDA, 1993.
- [27] W.P. Kustas, and D.C. Goodrich, "Preface to the special section on MONSOON'90," *Water Resour. Res.*, vol. 30, no. 5, pp. 1211-1225, 1994.
- [28] M.S. Moran, A.F. Rahman, J.C. Washburne, D.C. Goodrich, M.A. Weltz, and W.P. Kustas, "Combining the Penman-Monteith equation with measurements of surface temperature and reflectance to estimate evaporation rates of semiarid grassland," *Agr. For. Meteorol.*, vol. 80, pp. 87-109, 1996.
- [29] A. Beaudoin, M. Deshayes, L. Piet, N. Stussi, and T. Le Toan, "Retrieval and analysis of temperate forest backscatter signatures from multitemporal ERS-1 data over hilly terrain," *1st Symp. ERS-1 Pilot Project*, Toledo, Spain, 23-25 June 1994, pp. 283-289, 1994.
- [30] M.S. Moran, R.D. Jackson, P.N. Slater, and P.M. Teillet, "Evaluation of simplified procedures for retrieval of land surface reflectance factors from satellite sensor output," *Remote Sensing Environ.*, vol. 41, pp. 169-184, 1992.
- [31] J.C. Washburne, *A distributed surface temperature and energy balance model for a semiarid watershed*, Ph.D. Dissertation, University of Arizona, Department of Hydrology and Water Resources, 412 pp., 1994.
- [32] D. Troufleau, A. Vidal, A. Beaudoin, M.S. Moran, M.A. Weltz, D.C. Goodrich, J. Washburn, and A.F. Rahman, "Using optical-microwave synergy for estimating surface energy fluxes over semi-arid rangeland," in *Proc. 6th Int. Symp. Physical Measur.*

Signal. Remote Sensing, 17-21 Jan. 1994, Vald'Isere, France, 1994.

- [33] G.R. Blake, and K.H. Hartge, "Bulk density," *Methods of Soil Analysis*, Part 1, Physical and Mineralogical Methods, A. Klute, Ed. Madison, WN:ASA/SSA, Chap. 13, pp. 363-375, 2nd ed., 1986.
- [34] E.E. Sano, A.R. Huete, D. Troufleau, M.S. Moran, and A. Vidal, "Sensitivity analysis of ERS-1 synthetic aperture radar data to the surface moisture content of rocky soils in a semiarid rangeland", submitted to *Water Resour. Res.*

Table 1. Dates for the Acquisition of Remotely Sensed and Soil Moisture Data for the WG'92 Experiment.

Day of Year, 1992	Landsat TM	ERS-1 SAR	Soil Moisture Sampling
114	yes		yes
116		yes	
130			yes
135		yes	
146			yes
162	yes		yes
170		yes	
178	yes		yes
194	yes		
210			yes
226	yes		yes
240		yes	
258			yes
274	yes		yes
275		yes	
290			yes
291		yes	
306	yes		
310		yes	
326	yes		
206 ^a		yes	yes

^a Image acquired in 1994

Table 2. (a) Radar Backscattering Coefficients (dB), (b) Leaf Area Index, and (c) % Volumetric Soil Moisture Data from the Metflux Sites Located in the Shrub-dominated Sites of the Walnut Gulch Experimental Watershed (1992).

Day of Year	Metflux Sites				
	1	2	3	7	8
116	-10.61 ^(†)	-9.51	-9.15	-13.91	-10.42
135	-9.4	-8.85	-9.06	-12.97	-9.78
170	-11.79	-12.91	-11.09	-16.03	-12.7
240	-9.75	-10.05	-10.1	-9.66	-10.78
275	-8.49	-9.58	-9.42	-11.36	-10.66
291	-10.9	-11.1	-9.53	-13.81	-10.18
310	-8.3	-9.77	-9.72	-10.96	-10.96

(†) Radar backscattering coefficients (dB)

(a)

Day of Year	Metflux Sites				
	1	2	3	7	8
114	0.47 ^(††)	0.46	0.47	0.5	0.5
162	0.43	0.46	0.49	0.46	0.51
178	0.38	0.36	0.42	0.44	0.44
194	0.42	0.4	0.47	0.47	0.46
226	-	0.47	0.54	0.56	0.49
274	0.48	0.44	0.51	0.48	0.53
306	0.39	0.34	0.39	0.44	0.41
326	0.36	0.3	0.37	0.37	0.37

(††) Leaf Area Index values (unitless)

(b)

Table 2. *Continued*

Day of Year	Metflux Sites			
	1	3	5	6
114	2.75 ^(†††)	2.49	2.83	2.43
130	2.60	5.06	10.76	5.99
146	9.89	14.81	18.84	17.35
162	1.62	2.77	2.31	3.35
178	1.65	1.62	1.78	2.11
210	10.98	13.86	19.67	21.75
226	16.93	15.92	18.12	19.44
258	15.36	13.04	14.08	18.12
274	2.21	-	3.06	-
290	2.00	-	2.35	-

(†††) Volumetric soil moisture content (%)

(c)

Table 3. Synthetic Aperture Radar and Field Data from the 21 Validation Sites Located in the Shrub-dominated Part of the Walnut Gulch Experimental Watershed (1994 data).

Sampling Point	UTM (East-West)	UTM (North-South)	Backscattering Coefficient (dB)	Soil Moisture (g/g)
1	3512550	585919	-9.39	5.42
2	3511915	586178	-8.56	6.22
3	3511214	586882	-8.67	5.49
4	3509980	586177	-9.18	2.75
5	3510284	585769	-8.29	3.98
6	3505697	593802	-9.99	6.29
7	3506746	594404	-8.97	5.34
8	3507806	593359	-8.99	3.58
9	3507567	592558	-8.19	5.34
10	3511154	588333	-7.86	6.12
11	3513025	588458	-7.92	11.74
12	3512517	588488	-8.11	10.46
13	3512751	589841	-7.78	8.30
14	3511811	589109	-8.73	6.90
15	3512092	589711	-9.47	7.78
16	3511383	589706	-8.88	5.66
17	3511000	589044	-9.29	7.88
18	3512040	590393	-9.61	7.06
19	3511716	590388	-8.49	6.25
20	3510398	592299	-10.08	6.67
21	3508993	592309	-9.00	4.60

(after Sano et al. [29])

Table 3. *Continued*

Bulk Density (g/cm ³)	Soil Moisture (cm ³ /cm ³)	Biomass (g/m ²)	Rock Fragment (%)
1.50	8.13		
1.54	9.58	286	52
1.41	7.74		
1.43	3.93		
1.57	6.25	344	37
1.59	10.00	329	49
1.50	8.01	627	37
1.51	5.41		
1.48	7.90		
1.52	9.30		
1.60	18.78		
1.52	15.90	543	38
1.82	15.11		
1.68	11.59		
1.50	11.67		
1.68	9.51	415	27
1.47	11.58		
1.58	11.15	415	35
1.49	9.31		
1.64	10.94		
1.69	7.77	450	42

Table 4. Coefficients of Determination (r^2) Between Leaf Area Index and Radar Backscattering Coefficients for the Investigation Sites Located in the Shrub-dominated Sites of the Walnut Gulch Experimental Watershed (1992 data set).

Sampling Point	Coefficient of Determination (r^2)
1	0.64
2	0.60
3	0.49
4	0.44
5	0.50
6	0.50
7	0.00
8	0.01
9	0.01
10	0.24
11	0.28
12	0.37
13	0.65
14	0.55
15	0.75
16	0.36
17	0.52
18	0.85
19	0.46
20	0.47
21	0.47

FIGURE CAPTIONS

- Figure 1. Map of the Walnut Gulch Experimental Watershed showing its location in the State of Arizona.
- Figure 2. Temporal patterns of the backscattering coefficients and leaf area index for Metflux stations 1, 2, 3, 7, and 8.
- Figure 3. Scatterplot between radar backscattering coefficients and leaf area index for Metflux stations 1, 2, 3, 7, and 8. Numbers above symbols represent day of year in 1992. Number of samples $n = 5$. *S.E.* = Standard error.
- Figure 4. Scatterplot between radar backscattering coefficients corrected for topographic effects and leaf area index from Metflux stations 1, 2, and 7. Numbers above symbols represent the Metflux sites. The dashed lines correspond to the confidence interval of the linear regression at 95%. *S.E.* = standard error; n = number of samples.
- Figure 5. Scatterplot between radar backscattering coefficients and percent volumetric soil moisture content from Metflux sites 1 and 3 (a) without any correction for roughness and vegetation effects; (b) partially corrected for soil roughness effects; and (c) fully corrected for both roughness and vegetation effects. Numbers above symbols represent day of year in 1992.
- Figure 6. Temporal patterns of the backscattering coefficients and leaf area index for validation sites with r^2 values higher than 0.50. Numbers above the symbols represent day of year in 1992.
- Figure 7. Scatterplot between radar backscattering coefficients and soil moisture content for validation sites (a) without any correction for soil roughness and vegetation effects; (b) corrected for soil roughness effects; and (c) corrected for both soil roughness and vegetation effects. σ_0 = radar backscattering coefficient. The dashed lines correspond to the confidence interval of the linear regression at 95%. *S.E.* = standard error; number of samples $n = 7$.

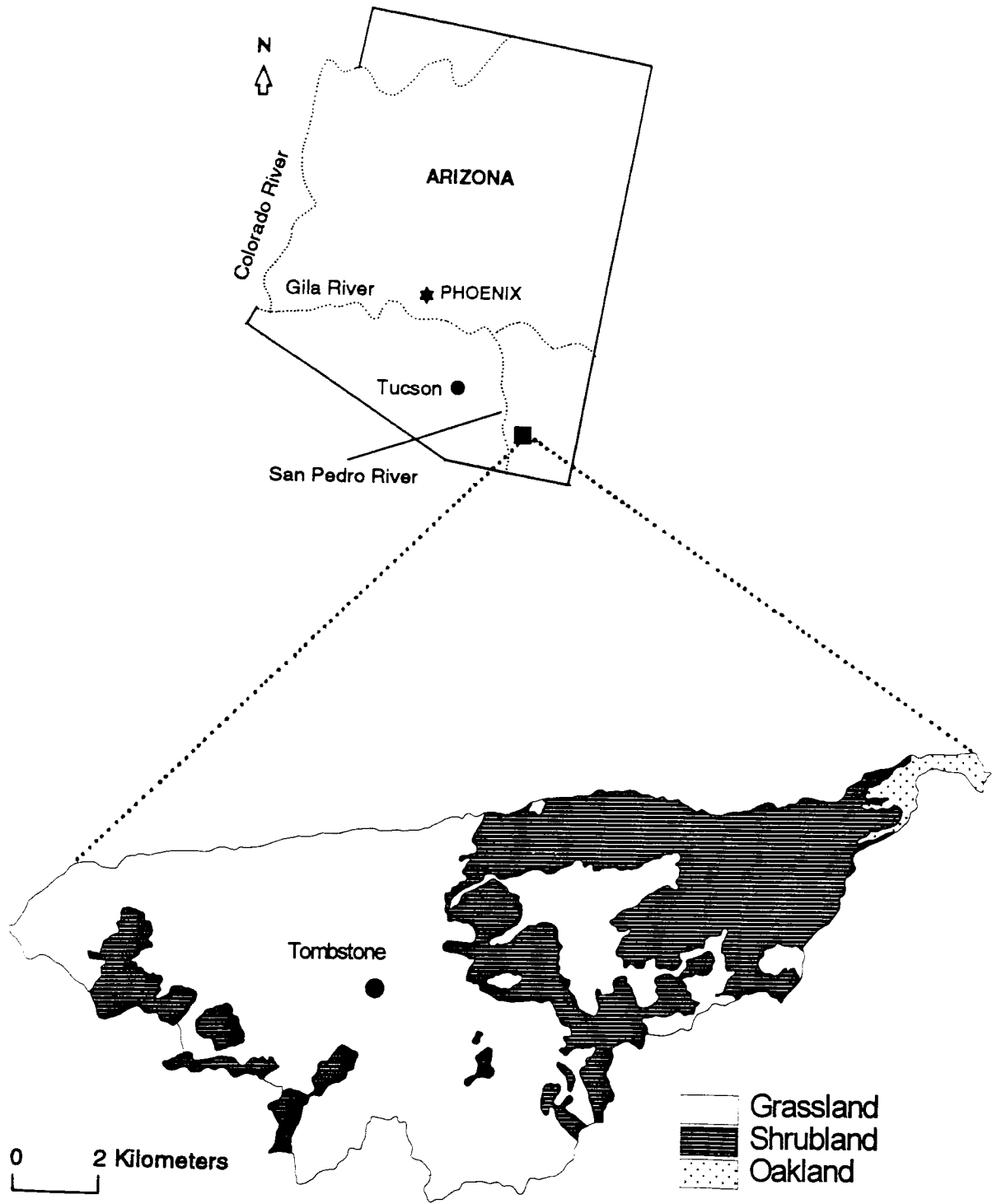


Figure 1

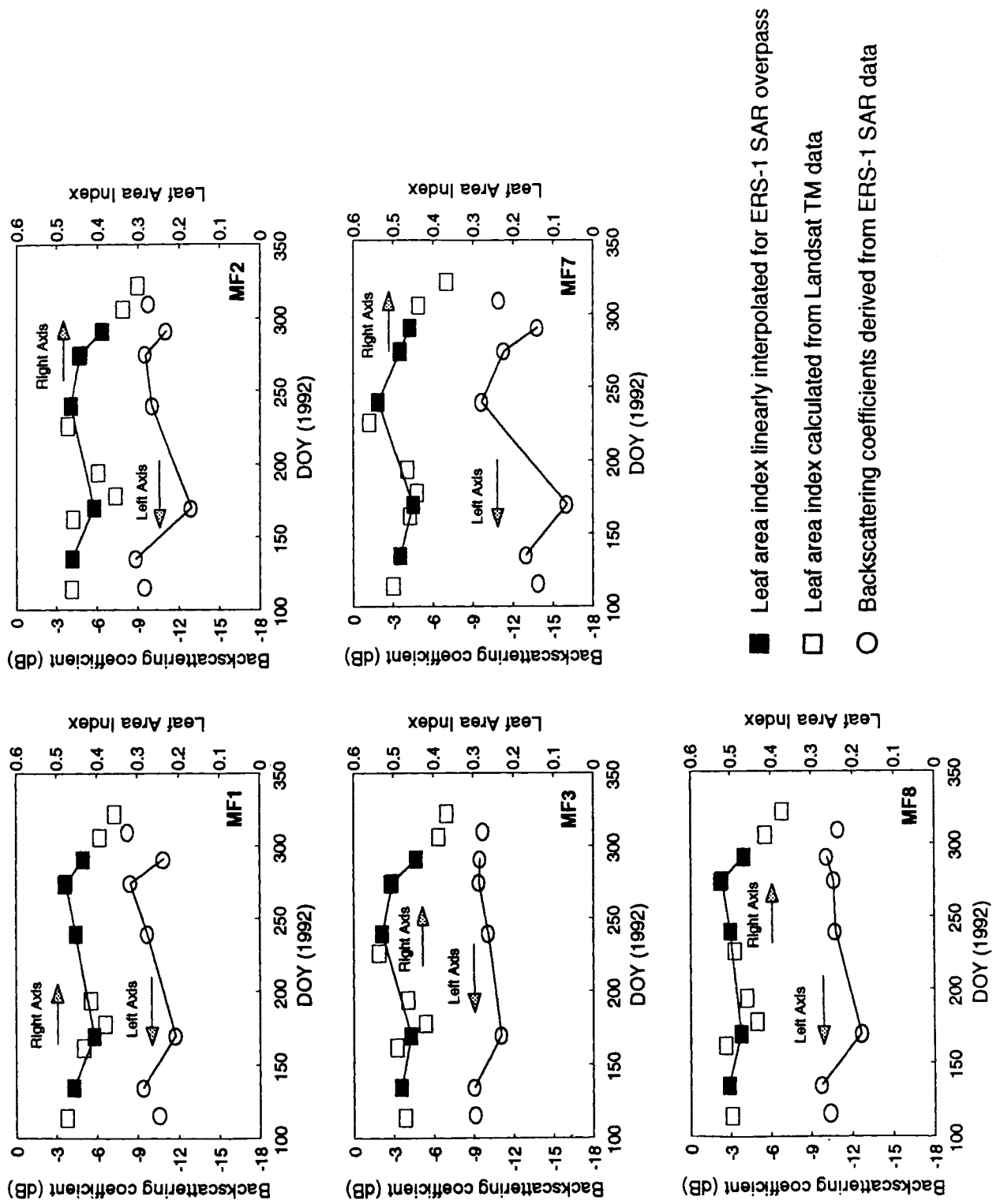


Figure 2

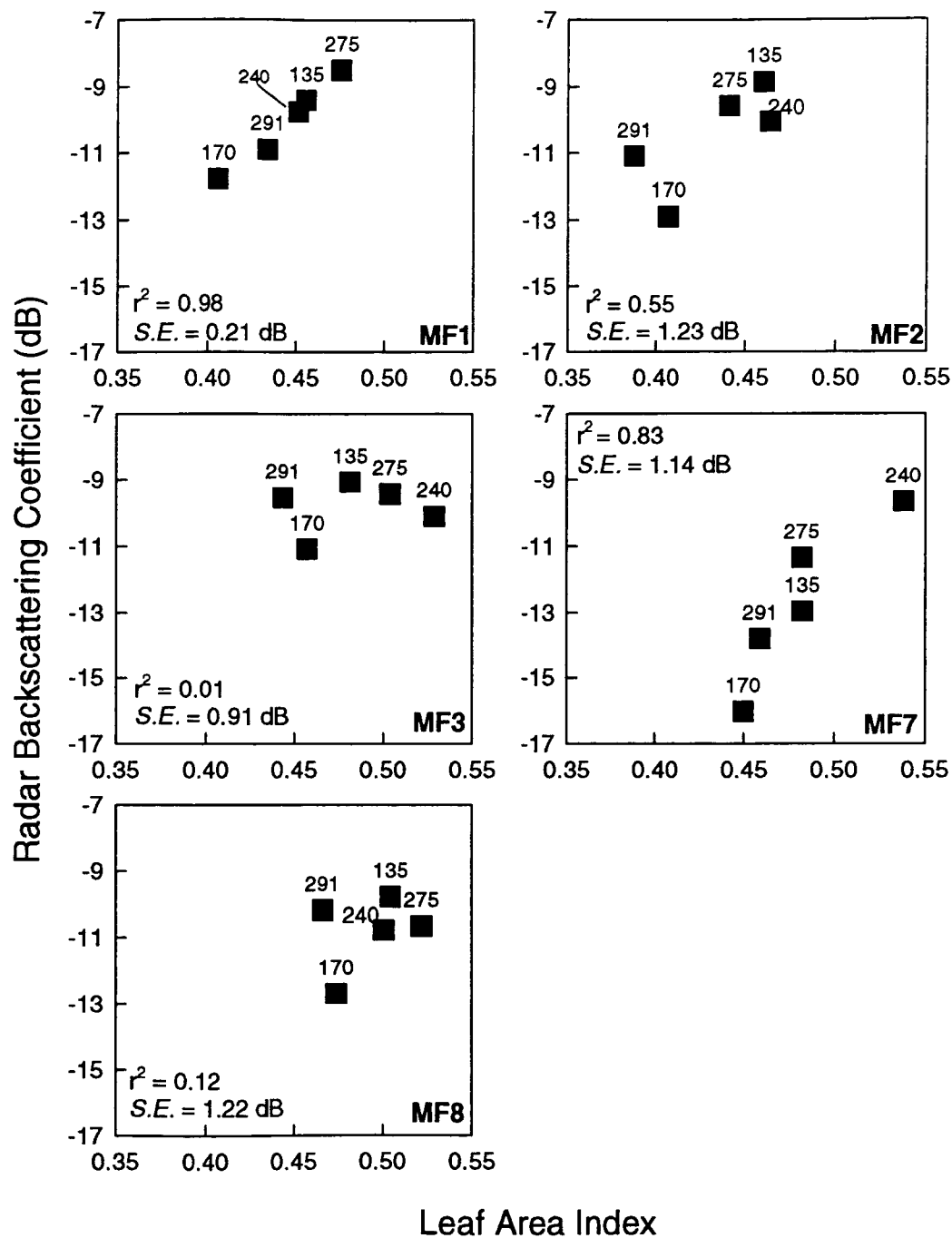


Figure 3

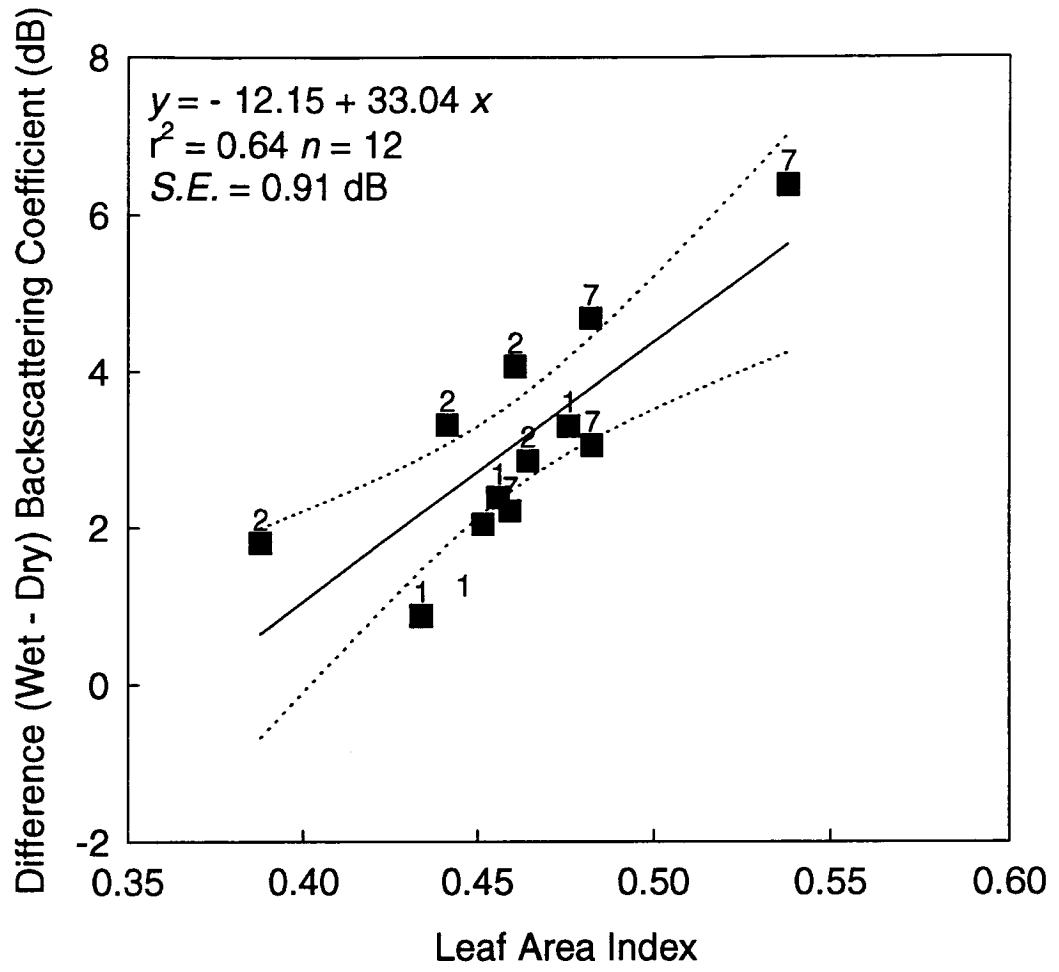


Figure 4

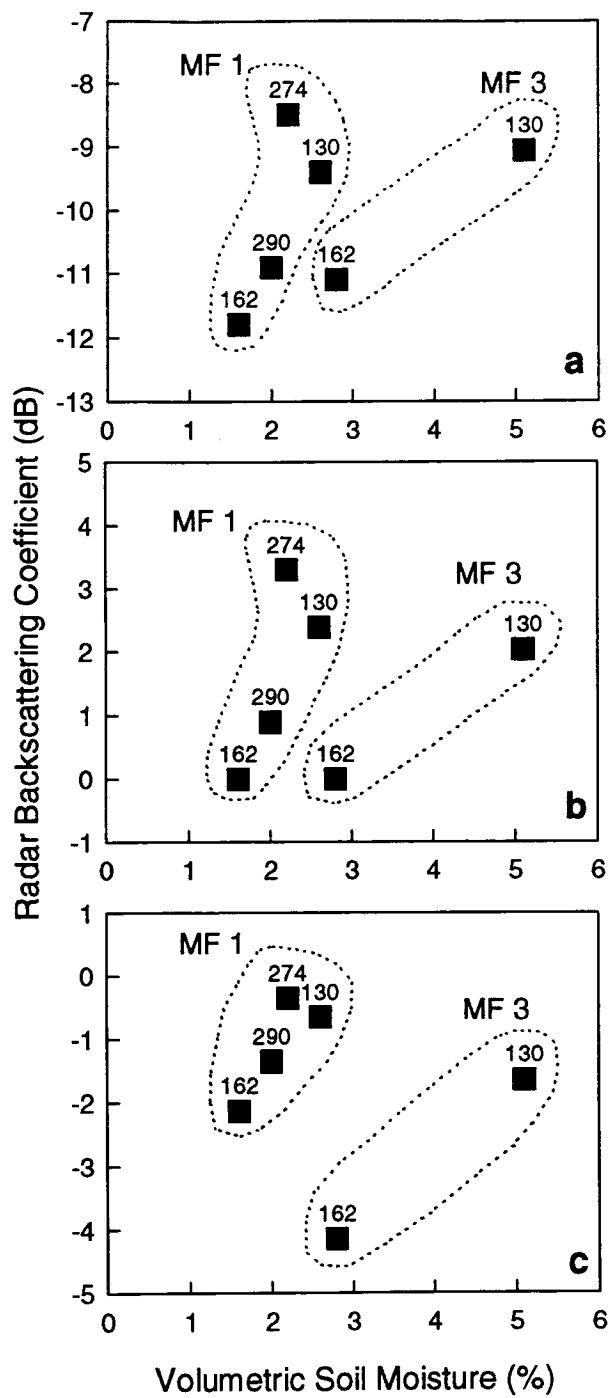


Figure 5

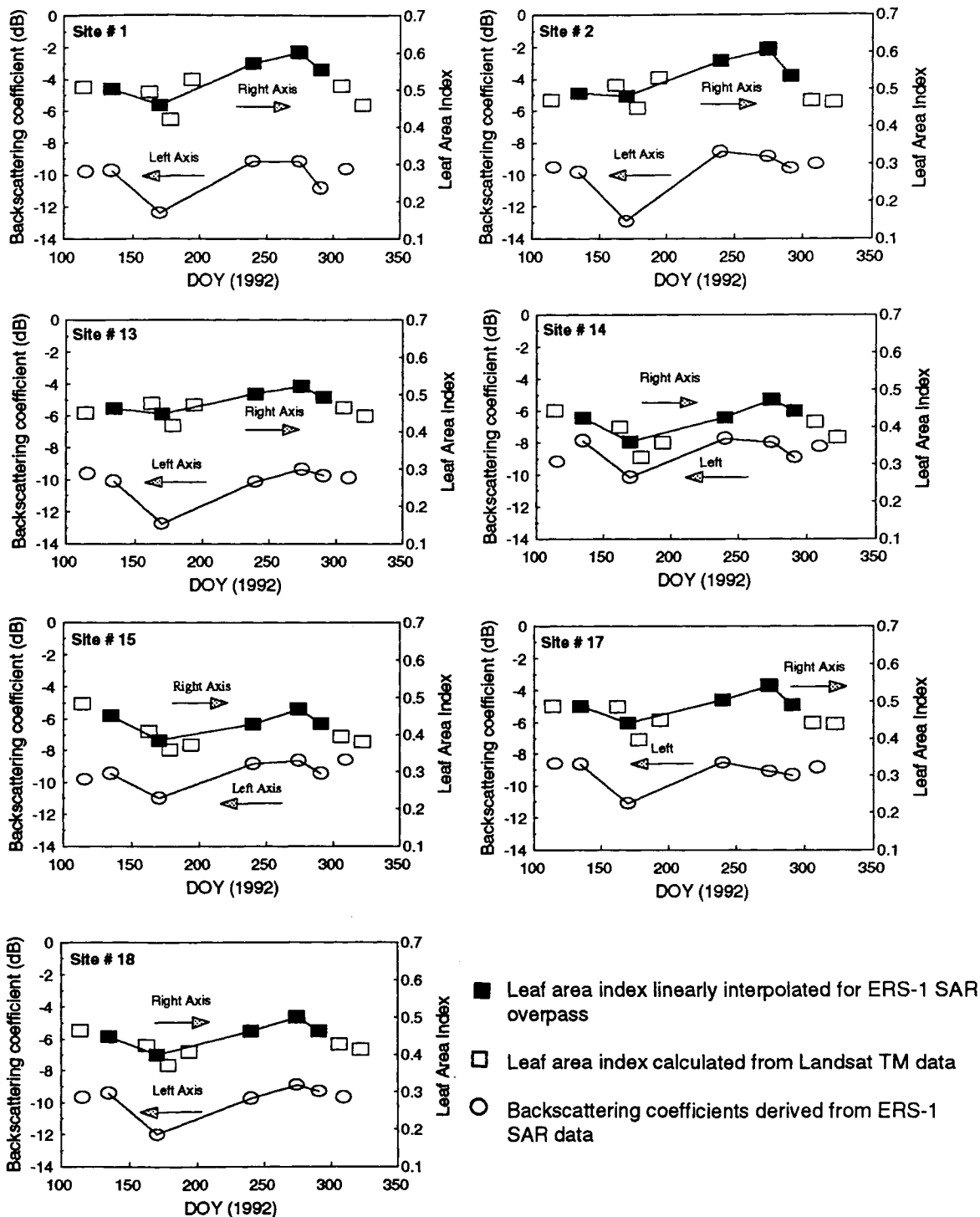


Figure 6

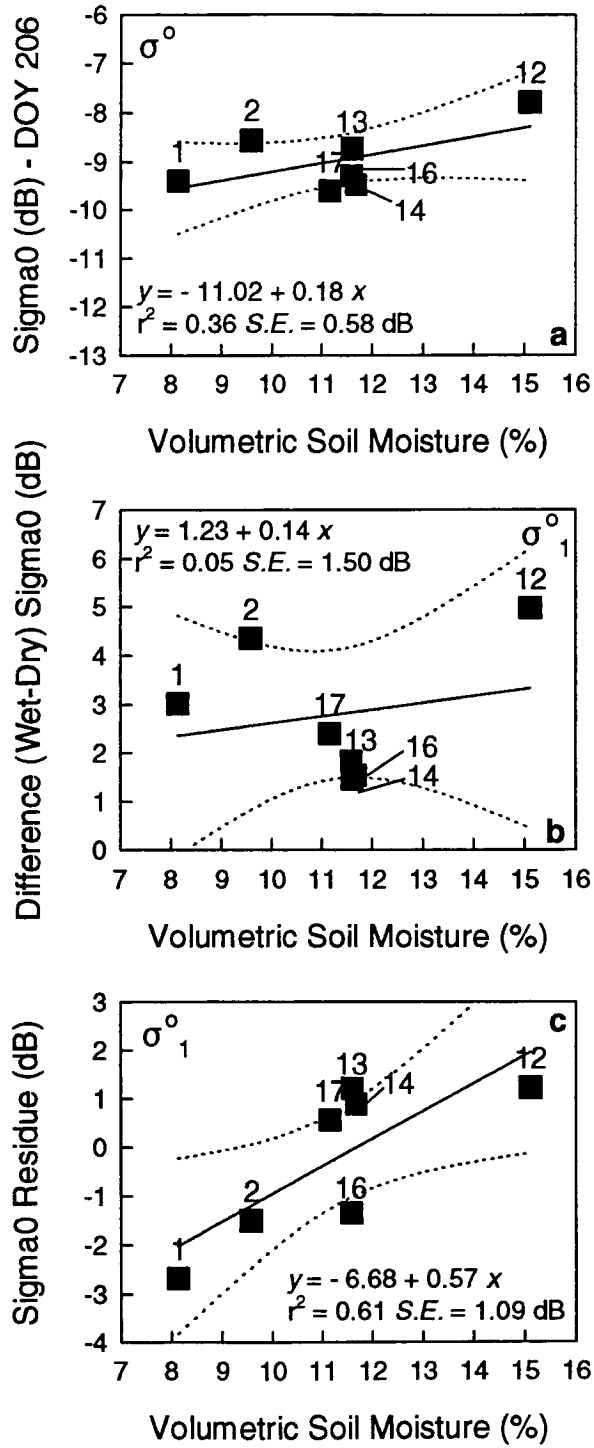


Figure 7

APPENDIX C:

C- and Multi-angle Ku-band Synthetic Aperture Radar Data for Bare Soil Moisture Estimation in Agricultural Areas

E.E. Sano¹, M.S. Moran², A.R. Huete¹, T. Miura¹

¹ Department of Soil, Water, and Environmental Science, The University of Arizona, 429 Shantz Bldg # 38, Tucson, Arizona, 85721, USA

² USDA-SWRC, 2000 E. Allen Road, Tucson, AZ, 85719, USA

Submitted to "Remote Sensing of Environment"

ABSTRACT

A sensitivity analysis of C-band (5.3 GHz) and Ku-band (14.85 GHz) synthetic aperture radar (SAR) data to the bare soil moisture content of agricultural fields was conducted in this study. The C-band data were obtained with a 23° incidence angle, whereas the Ku-band data were obtained with 35°, 55°, and 75° incidence angles. The fields presented either a small-scale or an intermediate-scale periodic soil roughness components, associated with level-basin and furrow irrigation systems, respectively. For fields with a small-scale roughness component, the SAR data were sensitive to soil moisture, particularly at the C-band with a 23° incidence angle and Ku-band with a 35° incidence angle. For fields with an intermediate-scale roughness component, both C- and Ku-band data were nearly insensitive to soil moisture. By using a theoretical surface scattering model, this study also analyzed the effects of different soil roughness components [root mean square (RMS) height h , correlation length, and periodic row structure] in the SAR data. For fields with RMS height < 0.3 cm, a small variation in h (from 0.1 to 0.3 cm) provoked a significant variation in the SAR data (up to 8 dB).

INTRODUCTION

Estimation of soil moisture in agricultural areas is important for improving yield forecasts, scheduling irrigations, and other farm management activities (Idso et al., 1975). Although conventional ground-based soil moisture measurement techniques, such as the neutron probe, Time Domain Reflectometry, and gravimetric methods, are accurate and

permit measurements of the entire soil profile, they are essentially point-based measurements at a specific time. On the other hand, remote sensing can provide indirect estimates over large areas with frequent repeat coverage. The microwave region (from 1 mm to 1 m wavelength) has been the most favorable spectral region for surface soil moisture studies (Schmugge, 1985; Engman and Chauhan, 1995). There is a large contrast between the dielectric constant ϵ of liquid water (~ 80) and dry soil (3-5) within this spectral range, which makes the synthetic aperture radar (SAR) data sensitive to soil moisture content (Ulaby et al., 1986; Engman and Chauhan, 1995).

For a bare soil surface, the radar backscattering process is controlled by the dielectric property of the soil, which is related to the soil moisture content, and the soil random surface roughness (Ulaby et al., 1978; Bernard et al., 1982; Dobson and Ulaby, 1986; Bertuzzi et al., 1992). One way to minimize the soil roughness influence is to use the co-polarized ratio technique; that is, the ratio between HH and VV polarized waves. Autret et al. (1989) and Chen et al. (1995) reported that SAR data derived from this technique are almost completely independent of soil roughness. However, these types of data have been collected by sensors mounted on airplanes or trucks and are available only at restricted experimental sites. No current spacecraft system has dual-polarization capability.

Another way to minimize the influence of soil roughness is to use data from sensors operating with a frequency and incidence angle around 5 GHz (C-band) and 10° , respectively (Ulaby and Bativala, 1976; Ulaby et al., 1978). However, to obtain high spatial resolutions (magnitude of tens of meters), satellites currently carrying SAR systems are configured with

incidence angles larger than the mentioned value: 23° for the European Remote Sensing (ERS-1, ERS-2) satellites; and 38° for the Japanese Earth Remote Sensing (JERS-1) satellite. The exception is the Canadian Remote Sensing (RADARSAT) satellite, which operates at 10° - 60° range of incidence angle.

Ulaby et al. (1978) showed that, depending upon the combination of frequency and incidence angle, the range of the radar backscattering coefficients σ° due to variations in surface roughness can vary up to 22 decibels (dB). In general, for smooth, bare soil surfaces with low soil moisture contents, σ° decreases rapidly with increasing incidence angle, particularly at angles close to nadir ($< 10^\circ$); conversely, for rough surfaces, σ° decreases gradually with increasing incidence angles. In addition, the concept of smooth and rough surface is frequency dependent. For instance, a soil surface appears rougher for sensors operating at 14.85 GHz (Ku-band) than for those operating at 5 GHz (C-band). The presence of periodic row or furrow structures in some agricultural sites can also exert considerable angular effects in the radar scattering process (Batlivala and Ulaby, 1976; Ulaby and Bare, 1979; Beaudoin et al., 1990). Thus, the sensitivity of the SAR data to soil moisture is sensor and site-specific. In other words, to obtain improved soil moisture estimates, the effects of soil roughness for a given sensor configuration and field condition need to be addressed by using either experimental data or theoretical/semiempirical models.

The objectives of this study were: a) to investigate the sensitivity of the C-band SAR data acquired at 23° incidence angle and the Ku-band SAR data acquired at three incidence angles (35°, 55°, and 75°) to the bare soil moisture content over agricultural fields with

different periodic row structures; and b) by using the theoretical surface scattering model developed by Ulaby et al. (1982a), investigate the sensitivity of SAR data to the following soil roughness components in the SAR data: root mean square (RMS) height h , correlation length L , and periodic row structure. The above mentioned sensor configurations were chosen because of their availability on existing aircraft and satellite platforms.

EXPERIMENTAL DESIGN

Site Description

The study site was at the University of Arizona's Maricopa Agricultural Center (MAC), a 770 hectare research and demonstration farm located south of Phoenix (33.08° N latitude, 111.98° W longitude), Arizona. Sandy loam, sandy clay loam, and clay loam are the predominant soil surface textures at the farm (Post et al., 1988). The major crop types consist of alfalfa grown year-round with 7 or 8 harvests per year; cotton, grown during the summer; and wheat, grown during the winter (Moran et al., 1996). Furrow and level-basin are the predominant irrigation systems.

The terrain was flat so that the geometric distortions in the radar data due to topographic effects were negligible. The rectangular-shaped fields are oriented in either North-South (N-S) or East-West (E-W) directions. Each field was subdivided into smaller areas defined as 'borders'. All fields selected contained the following structures produced by different tillage practices (Figure 1): a) a small-scale, periodic pattern associated with planting row structures with level-basin irrigation systems; or b) an intermediate-scale, periodic pattern

with furrow irrigation systems. These periodic structures were randomly perturbed by the presence of soil clods.

Synthetic Aperture Radar (SAR) Data

A set of airborne, 16-bit magnitude SAR images acquired on January 30, 1996, provided by the Sandia National Laboratories (SNL) in Albuquerque, New Mexico, were analyzed in this report. The sensor operated at 14.85 GHz (Ku-band) frequency, three incidence angles (35°, 55°, and 75°), VV polarization, and 2 meter nominal spatial resolution. The radar look-direction was N72°E. Another 16-bit amplitude SAR image acquired by the ERS-2 satellite on January 31, 1996 was also analyzed. This satellite operates at 5.3 GHz (C-band) frequency, 23° incidence angle, VV polarization, and 30 m nominal spatial resolution.

All images were georeferenced to the Universal Transverse Mercator coordinate system (zone 12, 1927 North American Datum, Clarke 1866). The total root mean square (RMS) errors of image registration were ~ 1.0 pixel for Ku-band and ~ 1.5 pixel for C-band. Radar backscattering coefficients (σ°) were extracted using the following equations:

$$\sigma^\circ (dB, C\text{-band}) = 10 \log (\overline{DN}^2 + STD^2) - K_1 \quad (1)$$

$$\sigma^\circ (dB, Ku\text{-band}) = 10 \log[(\overline{DN} + K_2)^2] \quad (2)$$

where DN is the digital number for each border; STD is the standard deviation; and K_1 and K_2 are the calibration constants (63.8 dB and 0.001426 dB, respectively). The averages and

standard deviations for the C- and Ku-band σ^0 calculations were obtained using at least 40 and 2000 pixels per border, respectively.

Ground-Based Measurements

A field survey was conducted on January 30, 1996, to record border-by-border qualitative estimates of the soil moisture and soil roughness conditions. The percent of crop cover was also registered. Based on this survey, the following fields were selected for ground truth measurements (Figure 2): a) fields with planting row structures: 18 (borders 1, 15, and 16); 23 (borders 6, 7, 8, and 9); 26 (borders 1, 5, 9, and 13); and 34 (all 16 borders); b) furrowed fields: 13 (borders 1, 2, 3 and 4); 21 (borders 1, 2, 5 and 6); 27 (borders 3 and 5); and 31 (borders 1 and 2).

These fields were characterized by bare soil or near-bare soil (less than 5 % of wheat cover) conditions and various soil roughness structures. The borders were selected taking into consideration the soil moisture variability within the field. Soil samples for gravimetric soil moisture measurements within the top 2 cm were collected in these fields during the Ku-band overpass. Because of the high homogeneity of the soil moisture condition within each border in the fields with planting row structures, one sample per border was collected at the center of the border. For the fields with furrow structures, three samples located at the bottom, middle and top of the furrows were collected and averaged for one reading. Volumetric soil moisture contents (Mv) were derived by assuming an average bulk density of 1.4 g/cm³ for the farm (D.F. Post, personal communication, 1996). This value is in the range of MAC's bulk

densities found by Post et al. (1988) for 0-30 cm depth (from 1.40 to 1.45 g/cm³).

Surface soil roughness was measured during the following days from the Ku-band overpass using a roughness meter consisting of a row of 100 equally spaced pins (Simanton et al., 1978). The device was aligned in the same radar look-direction (N72°E). Figure 3 shows an example of roughness sampling in fields with N-S planting row structure and E-W rough furrow structure, respectively. A total of 16 measurements per field were made for those with planting row structures. For furrowed fields, 32 measurements were collected per field; that is, two per border: one at the top of the furrow and another at the bottom of the furrow. The lines formed by 100 point readings were digitized in a Geographic Information System software package (Arc/Info) to calculate the roughness indices.

Theoretical Surface Backscattering Model at the MAC

The theoretical surface backscattering model used in this study is validated for randomly perturbed periodic surfaces and was developed by Ulaby et al. (1982a). The backscattering coefficients are derived by assuming that the scattering process is caused exclusively by the random part of the surface (Ulaby et al., 1986). The periodic component modulates the local slope α of the superimposed random component. Radar backscattering coefficients $\sigma^\circ(\theta)$ are calculated by:

$$\sigma^\circ(\theta) = \frac{1}{T} \int_0^T \sigma^\circ(\theta_1) \sec(\alpha) dy \quad (3)$$

where θ is the incidence angle of the sensor; T is the one spatial period of the row structure

(row spacing) in the direction y ; and θ_1 is the local incidence angle.

In practice, since the SAR resolution cell (~ 30 m for C-band and ~ 2 m for Ku-band) contains many row spatial periods (23.6 cm), $\sigma^\circ(\theta)$ is obtained by calculating a certain number of local backscatter coefficients $\sigma^\circ(\theta_1)$ over a differential segment dy and by integrating them along a spatial period T (Beaudoin et al., 1990). The term $\sigma^\circ(\theta_1)$ accounts for the scattering from the random component and the term $\sec(\alpha)$ accounts for the periodic component of the soil surface. The angles α and θ_1 are calculated by each segment dy as follows:

$$\alpha = \arctan \left[\frac{dR(y)}{dy} \right] \quad (4)$$

$$\theta_1 = \theta - \alpha \quad (5)$$

where $dR(y)$ is the relative height of the periodic component at a distance dy .

The Integral Equation Model (IEM) developed by Fung and Chen (1992) was used to estimate the $\sigma^\circ(\theta_1)$ values. The input data for the model are the wavelength λ , type of polarization, incidence angle of the sensor, dielectric constant ϵ , RMS height h , autocorrelation function $\rho(x')$, type of autocorrelation function, and correlation length L of the soil surface. Dielectric constants were derived from the following relation (Topp et al., 1980; Topp and Davis, 1985):

$$Mv = -0.0530 + 0.0292 \epsilon - 0.00055 \epsilon^2 + 0.0000043 \epsilon^3 \quad (6)$$

where Mv is the volumetric soil moisture content. This equation has been validated for a wide range of mineral soils and various soil moisture conditions (Altese et al., 1996).

The parameters h , $\rho(x')$, and L are related to the random soil roughness and were obtained from the height measurements using a device developed by Simanton et al. (1978). Because of the presence of the periodic components in these measurements, the random components were separated from the periodic components using the Fourier and the Inverse Fourier transforms. The RMS height h corresponded to the standard deviation of heights relative to a reference surface. The autocorrelation function for a spatial displacement $x' = (j-1)\Delta x$, where j is an integer ≥ 1 is given by (Ulaby et al., 1982b):

$$\rho(x') = \frac{\sum_{i=1}^{N-1} z_i z_{j,i-1}}{\sum_{i=1}^N z_i^2} \quad (7)$$

where z_i is the height z at a point i .

The surface correlation length L is defined as the displacement x' for which $\rho(x')$ is equal to $1/e$, that is:

$$\rho(L) = \frac{1}{e} \quad (8)$$

Fields 23 and 34 (planting row structures oriented approximately perpendicular to the radar beam direction) were selected to investigate the performance of the theoretical model for the sensor configurations analyzed in this study. Data from furrowed fields were not

analyzed because the IEM model used in this study was an approximation of the complete, but complex version. This approximate version is valid only for surfaces with small to moderate RMS heights or for low to medium frequencies (Altese et al., 1996). The following assumptions were made for the modeling: a) the influence of sparse vegetation cover (< 5% cover by wheat) in the radar backscattering process was negligible; and b) the influence of soil volumetric scattering was also considered negligible since SAR systems operating at high frequencies have a short penetration capability into the soils (~ 2 cm). The sensor configuration with the best performance was used to investigate the sensitivity of σ° to different soil roughness components in the scattering process. The criteria used to define the best performance was the Mean Absolute Difference (*MAD*):

$$MAD = | \sigma^\circ_{ESTIMATED} - \sigma^\circ_{MEASURED} | \quad (9)$$

where $\sigma^\circ_{ESTIMATED}$ refers to the σ° estimated by the model and $\sigma^\circ_{MEASURED}$ refers to the σ° measured by the SAR systems.

RESULTS

Field Data

Tables 1 and 2 summarize the field data obtained for this study. All fields were either bare soils or near bare soils with a maximum of 5% wheat cover. The volumetric soil moisture content ranged from 8 to 42%. The row spacing and amplitude for the fields with small scale row structures were 23.6 and 1.7 cm, respectively; for the intermediate-scale furrowed fields, the furrow spacing and amplitude were 95 and 22 cm, respectively.

Sensitivity of Measured SAR Backscatter to Soil Moisture

Figure 4 presents the scatterplot between radar backscattering coefficient σ° and % volumetric soil moisture content M_v for fields with a planting row structure. The test of significance for the correlation coefficients indicated that the correlations were significant at the 0.01 critical value. The highest slope (28.18) for the C-band at a 23° incidence angle indicated that this configuration was the best to estimate soil moisture. Among the Ku-band configurations, the 35° incidence angle was the best (slope = 23.71, $r^2 = 0.91$, for a confidence level of 95%), whereas the 75° incidence angle was nearly insensitive to the soil moisture. Despite an overall positive trend, the Ku-band at a 55° incidence angle was nearly insensitive to soil moisture when the latter was smaller than 25%. The sensitivity of σ° to the planting row direction was weak: for similar soil moistures, the σ° values from fields with N-S planting rows (Fields 23 and 34) were also approximately similar to those from fields with E-W planting rows (Fields 18 and 26).

Figure 5 shows the scatterplot between σ° and M_v from the furrowed fields. The backscattering coefficients from all borders with the same soil moisture contents within the same field were averaged. The σ° was insensitive to soil moisture for all sensor configurations, most likely because of the dominant influence of the soil roughness (presence of large soil clods, with a diameter higher than 15 cm, see Figure 2) in the backscattering process. We can also notice that the C-band backscatter coefficient was affected primarily by furrow direction. Regardless of the soil moisture content, the N-S oriented furrow structure of Field 31 presented the highest σ° values in this frequency.

Performance of the Theoretical Model: comparison with the experimental data

In this section, the performance of the theoretical model was verified by comparing the σ° derived by the model with the experimental data from Fields 23 and 34. The small-scale, periodic roughness pattern of these fields was found to be described by a cosine wave function with period $T = 23.6$ cm and amplitude $A = 1.7$ cm; that is:

$$y = 1.7 \cos \left(\frac{2\pi}{23.6} x + \pi \right) + 1.7 \quad (10)$$

Sixteen different values of α , one at each $dy = 1.5$ cm, were calculated to estimate $\sigma^\circ(\theta_1)$ (see Eq. 3). An example of ground profiles sampled by the roughness meter, its periodic components split from the random component using a Fourier and inverse Fourier transform, and its sinusoidal function modeled by Eq. 10, are shown in Figures 6a, 6b, and 6c, respectively. Regarding the random roughness component, the calculated autocorrelation function for the MAC data set was found to be closer to an exponential function, with a correlation length $L = 5$ and 6 cm for Fields 23 and 34, respectively. Previous studies (Fung et al., 1992; Oh et al., 1992) also showed that an exponential function was applicable to bare soil surfaces. Table 3 indicates the dielectric constant ϵ and the RMS height h values obtained from Fields 23 and 34. An average RMS height h of 0.3 cm for both fields was used to calculate $\sigma^\circ(\theta)$. The $\sigma^\circ(\theta)$ for the seven borders (10-16) of Field 34 for 35° and 75° incidence angle were not generated because measured SAR data were unavailable.

The model presented an overall underestimation for the Ku-band and an

overestimation for the C-band (Figure 7). The lowest mean absolute difference (*MAD*) was found for Ku-band with a 55° incidence angle (*MAD* = 2.6 dB), while the highest value was found for Ku-band with a 75° incidence angle (*MAD* = 5.5 dB). The C-band with a 23° incidence angle and the Ku-band with a 35° incidence angle presented intermediate differences (*MAD* = 3.67 and 4.10, respectively).

The weak performance of the model was provoked by the high sensitivity of the IEM to the soil roughness, as already reported by Altese et al. (1996). Thus, a small error in the RMS height calculation can affect the σ° derivation significantly. For instance, the *MAD* for Ku-band with a 55° incidence angle can be reduced by its half value (from 2.6 dB to 1.3 dB) if we use $h = 0.4$ cm, instead of 0.3 cm. Therefore, the accuracy of the RMS height measurements is the key issue to obtain an accurate soil moisture retrieval from inversion procedures.

Sensitivity of the model to different soil roughness components

Because of its lowest mean average difference, the Ku-band with a 55° incidence angle was chosen to investigate the sensitivity of σ° to the different soil roughness components (RMS height, correlation length, and periodic row spacing). The results are shown in Table

4. We can notice that:

1. the sensitivity of σ° to the soil surface roughness was significant, particularly for fields with RMS height $h < 0.3$ cm. A variation of h from 0.1 cm to 0.3 cm provoked a variation in σ° of ~ 9 dB. The RMS height influence decreased significantly when h was higher than

- 0.3 cm (σ° variation of ~ 3 dB for a variation in h from 0.3 to 0.5 cm).
2. the sensitivity of σ° to the soil moisture was independent of roughness condition. A variation of ~ 9 dB was found for a soil moisture variation from 5 to 45%, regardless of soil roughness condition.
 3. for fields with $h < 0.3$ cm, the sensitivity of σ° to the soil roughness is much higher than the sensitivity to the soil moisture. A variation in RMS height from 0.1 cm to 0.3 cm provoked the same magnitude of σ° variation for a soil moisture variation from 5 to 45%.
 4. the sensitivity of the σ° to the correlation length L was low. The σ° variation due to an increment of 2 cm in L was < 1.7 dB.
 5. the sensitivity of σ° to the periodic row structure was not significant. The effect of periodic planting row structures in the σ° derivation was < 0.6 dB.

CONCLUDING REMARKS

The results of this investigation presented two opposite results. SAR data from MAC was sensitive to the soil moisture for fields with planting row structures, particularly for the C-band with a 23° incidence angle and the Ku-band with a 35° incidence angle. The direction of the small-scale, periodic roughness components did not present any influence in the scattering process, regardless of frequency and sensor incidence angle. For the Ku-band with a 55° incidence angle, the radar data were nearly insensitive to the soil moisture when the latter was smaller than 25%. However, for furrowed fields, the SAR data from all configurations analyzed in this study were insensitive to soil moisture content. The relatively

large, randomly distributed soil clods in the furrowed fields most likely played a major role in the radar backscattering process. The influence of the furrow direction was verified only at the C-band configuration, where the σ° values from N-S oriented furrowed fields were higher than from any other E-W oriented fields, regardless of soil moisture content.

Therefore, the estimation of soil moisture from furrowed fields using SAR data operating at a single polarization and a single frequency seems to be difficult, unless some technique to reduce the effects of soil roughness is applied. Sano et al. (1997) obtained an improved soil moisture estimation from a rocky soil in a semiarid region by subtracting wet season σ° from a dry season σ° . The assumption was that the SAR data from a dry season was dependent only on the soil roughness. This technique, upon validation, can be an easy way to reduce the soil roughness effects and should be also tested in agricultural fields.

The performance of the theoretical model was relatively weak because of the high sensitivity of the IEM to the soil roughness, particularly for fields with RMS height < 0.3 cm. Therefore, in such roughness conditions, the inversion of σ° to the soil moisture is not reliable without an accurate information of soil roughness. Research to determine the number of soil roughness samples necessary to obtain accurate RMS heights needs to be conducted. Results from this study and from Altese et al. (1996) suggest that an accuracy of ± 0.01 cm in RMS height calculation should be considered.

The IEM used in this study was an approximate model of its complete version. The complete version describes the backscattering process without any limitation on roughness or frequency, whereas the approximate version is valid for surfaces with small to moderate

RMS heights or for low to medium frequencies (Altese et al., 1996). Despite its complexity, the complete version of IEM should be considered in the future to investigate the influence of different soil roughness parameters in MAC furrowed fields or in any other farm with similar field conditions.

ACKNOWLEDGMENTS

The authors wish to thank Tom Mitchell for his help in processing the SAR images. Jiaguo Qi and Ed Barnes provided assistance in the field soil roughness and moisture content measurements. Special thanks to Dr. T.J. Jackson, Dr. S. Yool, and Dr. D. Troufleau for useful suggestions. Partial support for this research was provided by the National Science Foundation (INT-9314872). We are also grateful to personnel at the Maricopa Agricultural Center (MAC), for their assistance and cooperation.

REFERENCES

- Altese, E., Bolognani, O., Mancini, M., and Troch, P.A. (1996), Retrieving soil moisture over bare soil from ERS 1 synthetic aperture radar data: Sensitivity analysis based on a theoretical surface scattering model and field data, *Water Resour. Res.* 32(3):653-661.
- Autret, M., Bernard, R., and Vidal-Madjar, D. (1989), Theoretical study of the sensitivity of the microwave backscattering coefficient to the soil surface parameters, *Int. J. Remote Sens.* 10(1):171-179.
- Batlivala, P.P., and Ulaby, F.T. (1976), Radar look direction and row crops, *Photogramm. Eng. Remote Sens.* 42(2):233-238.

- Beaudoin, A., LeToan, T., and Gwyn, Q.H.J. (1990), SAR observations and modeling of the C-band backscatter variability due to multiscale geometry and soil moisture, *IEEE Trans. Geosci. Remote Sens.* 28(5):886-895.
- Bernard, R., Martin, P.H., Thony, J.L., Vauclin, M., and Vidal-Madjar, D. (1982), C-band radar for determining surface soil moisture, *Remote Sens. Environ.* 12:189-200.
- Bertuzzi, P., Chanzy, A., Vidal-Madjar, D., and Autret, M. (1992), The use of a microwave backscatter model for retrieving soil moisture over bare soil, *Int. J. Remote Sens.* 13:2653-2668.
- Chen, K.S., Yen, S.K., and Huang, W.P. (1995), A simple model for retrieving bare soil moisture from radar-scattering coefficients, *Remote Sens. Environ.* 54:121-126.
- Dobson, M.C., and Ulaby, F.T. (1986), Active microwave soil moisture research, *IEEE Trans. Geosci. Remote Sens.* 24:23-36.
- Engman, E.T., and Chauhan, N. (1995), Status of microwave soil moisture measurements with remote sensing, *Remote Sens. Environ.* 51:189-198.
- Fung, A.K., and Chen, K.S. (1992), Dependence of backscattering coefficients on frequency, roughness, and polarization states, *Int. J. Remote Sens.* 13(9):1663-1680.
- Fung, A.K., Li, Z., and Chen, K.S. (1992), Backscattering from a randomly rough dielectric surface, *IEEE Trans. Geosci. Remote Sens.* 30(2):356-369.
- Idso, S.B., Jackson, R.D. and Reginato, R.J. (1975), Detection of soil moisture by remote surveillance, *Amer. Sci.* 63:549-557.
- Moran, M.S., Vidal, A., Troufleau, D., Qi, J., Clarke, T.R., Pinter, Jr., P.J., Mitchell, T.A., Inoue, Y., and Neale, C.M.U. (1997), Combining multifrequency microwave and optical data for farm management, *Remote Sens. Environ.* (in press).

- Oh, Y., Sarabandi, K., and Ulaby, F.T. (1992), An empirical model and an inversion technique for radar scattering from bare soil surfaces, *IEEE Trans. Geosci. Remote Sens.* 30(2):370-381.
- Post, D.F., Mack, C., Camp, P.D., and Suliman, A.S. (1988), Mapping and characterization of the soils on the University of Arizona Maricopa Agricultural Center, *Hydrology and Water Resources in Arizona and the Southwest*, American Water Resources Association/Arizona-Nevada Academy of Science, Tucson, AZ, Vol. 18, pp. 49-60.
- Sano, E.E., Huete, A., Troufleau, D., Moran, M.S., and Vidal, A. (1997), Sensitivity analysis of ERS-1 synthetic aperture radar data to the surface moisture content of rocky soils in a semiarid rangeland, *Water Resour. Res.* (submitted).
- Schmugge, T. (1985), Remote Sensing of soil moisture, In *Hydrological Forecasting* (M.G. Anderson and T.P. Burt, Eds.), John Wiley & Sons Ltd., New York, pp. 101-123.
- Simanton, J.R., Dixon, R.M., and McGowan, I. (1978), A microroughness meter for evaluating rainwater infiltration, *Hydrology and Water Resources in Arizona and the Southwest*, American Water Resources Association, Arizona-Nevada Academy of Science, Tucson, AZ, Vol. 8, pp. 171-174.
- Topp, G.C., and Davis, J.L. (1985), Measurements of soil water content using time domain reflectometry: A field evaluation, *Soil Sci. Am. J.* 49:19-24.
- Topp, G.C., Davis, J.L., and Annan, A.P. (1980), Electromagnetic determination of soil water content: Measurement in coaxial transmission lines, *Water Resour. Res.* 16:574-582.
- Ulaby, F.T., and Batlivala, P.P. (1976), Optimum radar parameters for mapping soil moisture, *IEEE Trans. Geosci. Electron.* 14(2):81-93.
- Ulaby, F.T., Batlivala, P.P., and Dobson, M.C. (1978), Microwave backscatter dependence on surface roughness, soil moisture and soil texture: Part I - bare soil, *IEEE Trans. Geosci. Electron.* 16(4):286-295.

- Ulaby, F.T., and Bare, J.E. (1979), Look direction modulation function of the radar backscattering coefficient of agricultural fields, *Photogramm. Engin. Remote Sens.* 45(11):1495-1506.
- Ulaby, F.T., Kouyate, F., Fung, A.K., and Sieber, A.J. (1982a), A backscatter model for a randomly perturbed periodic surface, *IEEE Trans. Geosci. Remote Sens.* 20:518-528.
- Ulaby, F.T., Moore, R.K., and Fung, A.K. (1982b), *Microwave remote sensing. Active and passive*, Addison-Wesley, Reading, MA, Vol. II, Chap. 11, pp. 816-921.
- Ulaby, F.T., Moore, R.K., and Fung, A.K. (1986), *Microwave remote sensing: Active and Passive*, Artech House, Dedham, MA, Vol. III, Chap. 21, pp. 1797-1999.

Table 1. Field Data from Maricopa Agricultural Center Acquired on January 30 and 31, 1996: Fields with Planting Row Structure.

Field	Border	Row Direction	Crop Cover	Volumetric Soil Moisture Content (%)
18	1	E-W	Wheat (< 3 %)	42
	15			10
	16			14
23	6	N-S	Wheat (< 5 %)	36
	7			35
	8			13
	9			10
26	1	E-W	Wheat (< 1 %)	10
	5			11
	9			8
	13			10
34	1	N-S	Wheat (< 1 %)	24
	2			20
	3			15
	4			15
	5			15
	6			14
	7			14
	8			20
	9			20
	10			24
	11			29
	12			31
	13			36
	14			34
	15			32
	16			35

Table 2. Field Data from Maricopa Agricultural Center Acquired on January 30 and 31, 1996: Furrowed Fields.

Field	Border	Furrow Direction	Crop Cover	Volumetric Soil Moisture Content (%)
13	1	E-W	Bare Soil	8
	2			8
	3			7
	4			8
21	1	E-W	Wheat (< 5 %)	25
	2			20
	5			8
	6			8
27	3	E-W	Wheat (< 1 %)	34
	5			20
31	1	N-S	Bare Soil	24
	2			11

Table 3. Dielectric Constant and RMS Height Data Calculated for Fields 23 and 34.

Field	Border	Dielectric Constant	RMS height (cm)
23	5	21	0.3
	6	20	0.3
	7	7	0.2
	8	6	0.3
34	1	13	0.2
	2	11	0.3
	3	8	0.4
	4	8	0.3
	5	8	0.2
	6	8	0.3
	7	8	0.3
	8	11	0.2
	9	11	0.2
	10	13	0.4
	11	16	0.3
	12	17	0.3
	13	21	0.5
	14	20	0.3
	15	18	0.3
	16	20	0.3

Table 4. Influence of (a) RMS Height h , (b) Correlation Length L , and (c) Periodic Row Structure in the Surface Scattering Process for the Ku-band with a 35° Incidence Angle.

Soil Moisture (%)	Dielectric Constant	RMS height h (cm)				
		$h_1 = 0.1$	$h_2 = 0.3$	$h_3 = 0.5$	$h_2 - h_1$	$h_3 - h_2$
5	3.8	-29.29	-20.75	-18.08	8.54	2.67
10	5.8	-26.67	-18.06	-15.23	8.61	2.83
15	8.1	-25.02	-16.36	-13.43	8.66	2.93
20	10.6	-23.90	-15.20	-12.20	8.70	3.00
25	13.4	-23.03	-14.31	-11.26	8.72	3.05
30	16.6	-22.32	-13.58	-10.50	8.74	3.08
35	20.4	-21.70	-12.95	-9.83	8.75	3.12
40	25.0	-21.14	-12.38	-9.24	8.76	3.14
45	30.8	-20.62	-11.85	-8.69	8.77	3.16
(Highest - Lowest) Difference	27.0	8.67	8.90	9.39		

(a)

Table 4. - *Continued*

Soil Moisture (%)	Dielectric Constant	RMS height h (cm)				
		$h_1 = 0.1$	$h_2 = 0.3$	$h_3 = 0.5$	$h_2 - h_1$	$h_3 - h_2$
5	3.8	-19.04	-20.75	-21.99	1.71	1.24
10	5.8	-16.35	-18.06	-19.29	1.71	1.23
15	8.1	-14.65	-16.36	-17.59	1.71	1.23
20	10.6	-13.49	-15.20	-16.43	1.71	1.23
25	13.4	-12.60	-14.31	-15.54	1.71	1.23
30	16.6	-11.87	-13.58	-14.81	1.71	1.23
35	20.4	-11.24	-12.95	-14.18	1.71	1.23
40	25.0	-10.37	-12.38	-13.61	2.01	1.23
45	30.8	-10.14	-11.85	-13.08	1.71	1.23
(Highest - Lowest) Difference	27.0	8.90	8.90	8.91		

(b)

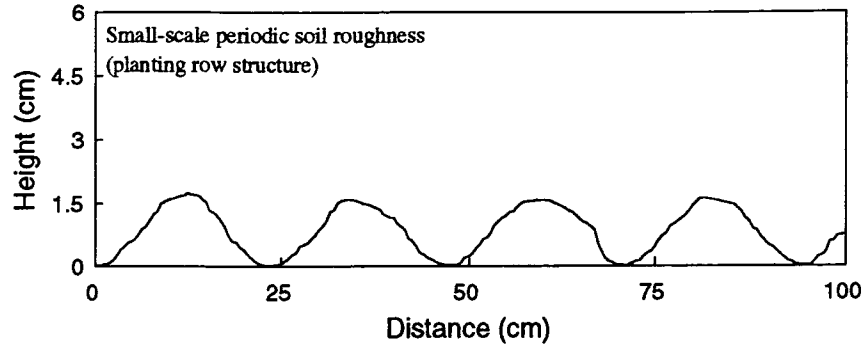
Table 4. - *Continued*

Soil Moisture (%)	Dielectric Constant	Contribution (dB) from Soil Clods (S_1) ^a	Contribution (dB) from Soil Clods and Row Structures (S_2) ^b	$S_2 - S_1$
5	3.8	-21.32	-20.75	0.57
10	5.8	-18.56	-18.06	0.50
15	8.1	-16.82	-16.36	0.46
20	10.6	-15.62	-15.2	0.42
25	13.4	-14.71	-14.31	0.40
30	16.6	-13.96	-13.58	0.38
35	20.4	-13.31	-12.95	0.36
40	25.0	-12.73	-12.38	0.35
45	30.8	-12.19	-11.85	0.34
(Highest - Lowest) Difference	27.0	9.13	8.90	

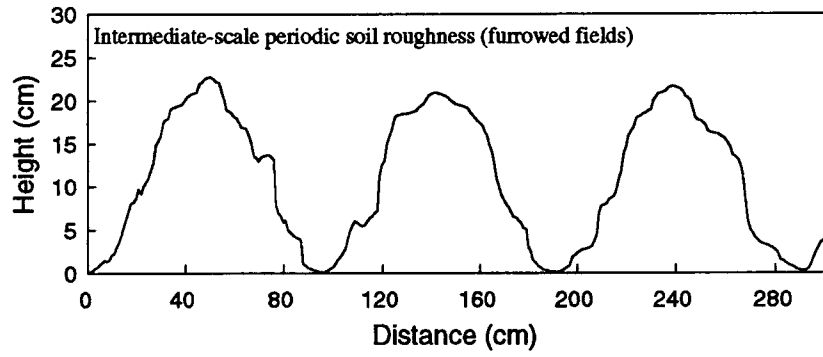
^a Calculated from Integral Equation Model
^b Calculated from Ulaby et al. (1982a) model

FIGURE CAPTIONS

- Figure 1. Schematic soil surface roughness components of Maricopa Agricultural Center fields, (a) small-scale periodic roughness;(b) intermediate-scale periodic roughness.
- Figure 2. C-band ERS-2 SAR image of Maricopa Agricultural Center with fields selected for ground truth measurements.
- Figure 3. Examples of soil roughness measurements, (a) Field 34, border 2, with approximately North-South planting row structure; and (b) Field 21, border 2, with approximately East-West furrow structure.
- Figure 4. Scatterplot between SAR data and % volumetric soil moisture content for fields with planting row structure, (a) the Ku-band with a 35° incidence angle; (b) the Ku-band with a 55° incidence angle; (c) the Ku-band with a 75° incidence angle; and (c) the C-band with a 23° incidence angle. 1 = Field 18; 2 = Field 23; 3 = Field 26; 4 = Field 34. The dashed lines correspond to the confidence interval of the linear regression at 95%. *S.E.* = standard error; *n* = number of samples.
- Figure 5. Scatterplot between SAR data and % volumetric soil moisture content for furrowed fields, (a) the Ku-band with a 35° incidence angle; (b) the Ku-band with a 55° incidence angle; (c) the Ku-band with a 75° incidence angle; and (c) the C-band with a 23° incidence angle. 1 = Field 13; 2 = Field 21; 3 = Field 27; 4 = Field 31. The dashed lines correspond to the confidence interval of the linear regression at 95%. *S.E.* = standard error; *n* = number of samples.
- Figure 6. Example of (a) ground profile sampled in the field, (b) its periodic roughness component, and (c) its sinusoidal function. Data from Field 34, border 5.
- Figure 7. Scatterplot between modeled and measured radar backscattering coefficients.

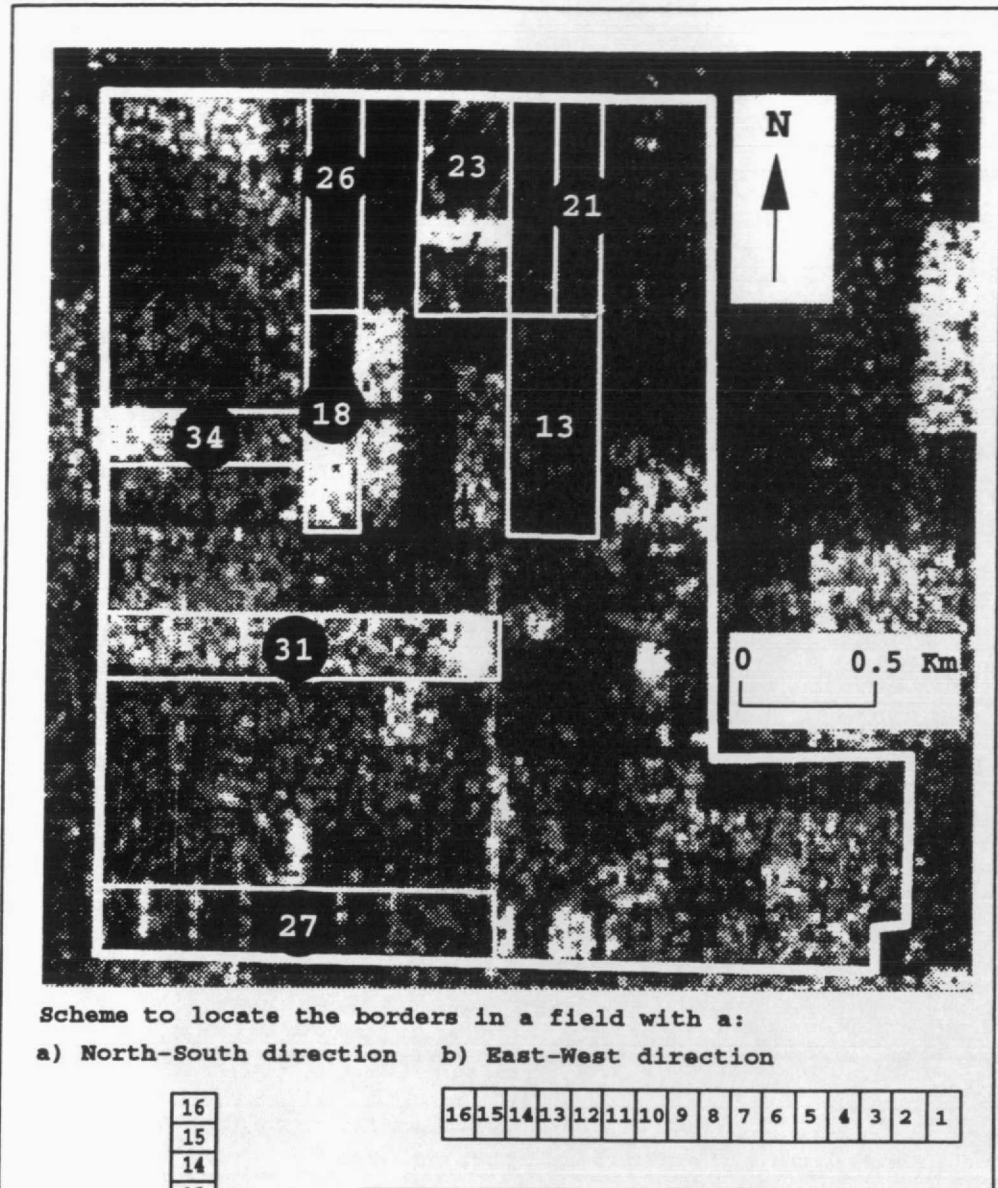


(a)



(b)

Figure 1



Location of the study area at state level:

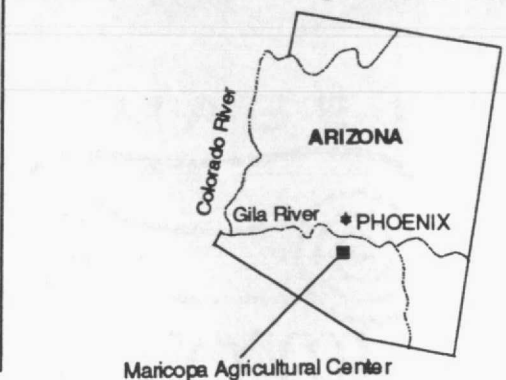


Figure 2



(a)



(b)

Figure 3

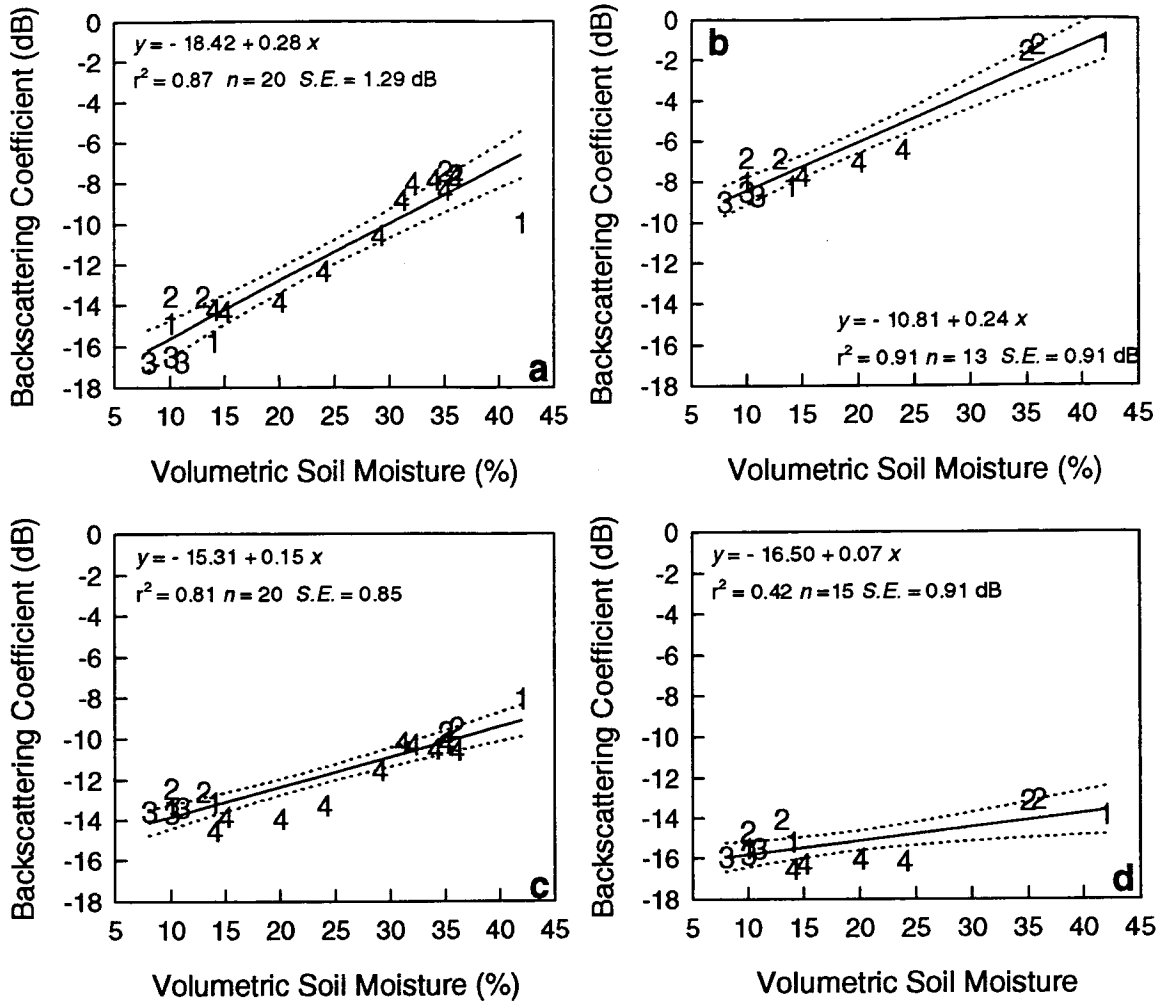


Figure 4

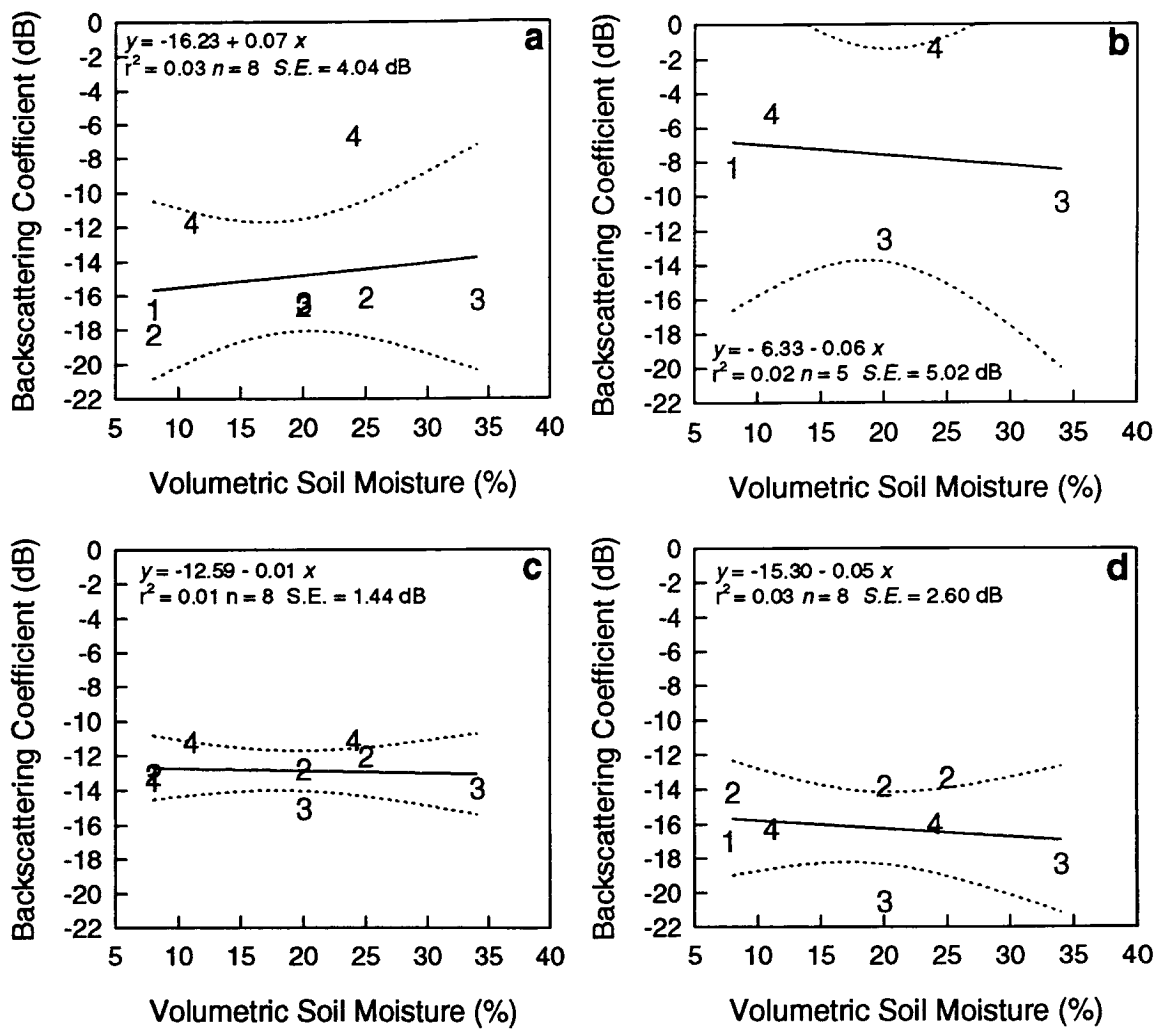


Figure 5

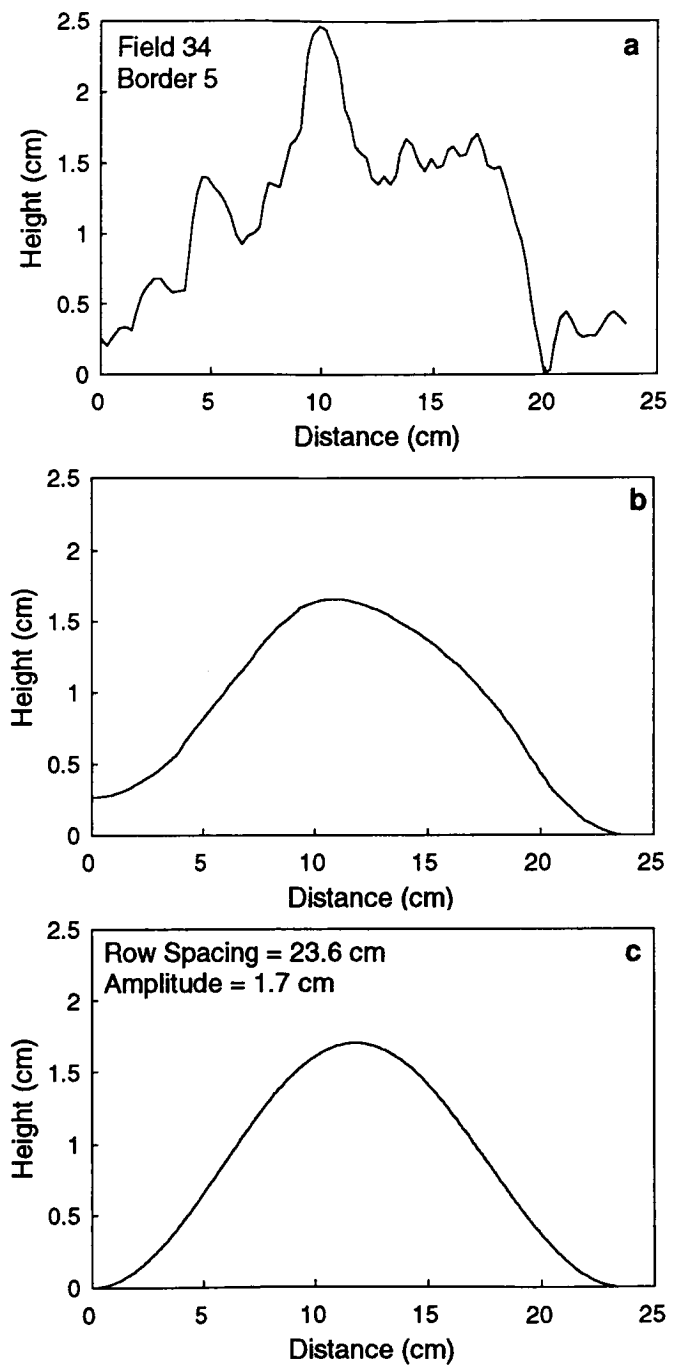


Figure 6

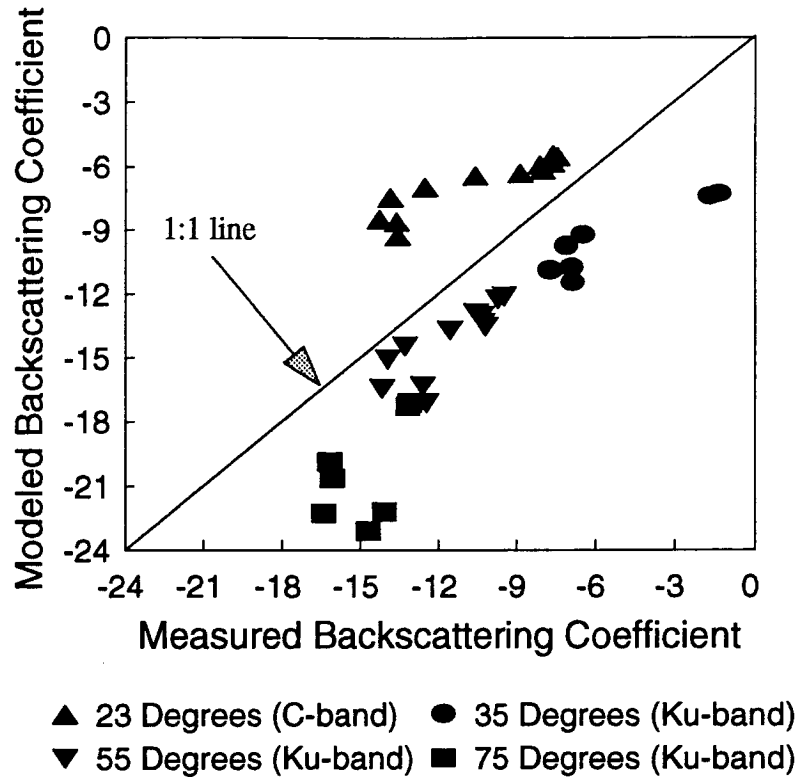


Figure 7